Journal of Experimental Marine Biology and Ecology 532 (2020) 151444

Contents lists available at ScienceDirect

Journal of Experimental Marine Biology and Ecology

journal homepage: www.elsevier.com/locate/jembe

Response of a natural Antarctic phytoplankton assemblage to changes in temperature and salinity

Julieta S. Antoni[a,b,*], Gastón O. Almandoz[a,b], Martha E. Ferrario[a,b], Marcelo P. Hernando[c], Diana E. Varela[d], Patrick D. Rozema[e], Anita G.J. Buma[e], Flavio E. Paparazzo[f,g], Irene R. Schloss[b,h,i]

[a] División Ficología, Facultad de Ciencias Naturales y Museo, Universidad Nacional de La Plata, 1900 La Plata, Argentina
[b] CONICET, Argentina
[c] Departamento de Radiobiología, Comisión Nacional de Energía Atómica, 1650 San Martín, Buenos Aires, Argentina
[d] Department of Biology, and School of Earth and Ocean Sciences, University of Victoria, Victoria B.C. V8W 2Y2, Canada
[e] Department of Ocean Ecosystems, ESRIG, University of Groningen, Groningen 9747 AG, the Netherlands
[f] Centro para el Estudio de Sistemas Marinos, CESIMAR-CONICET, Brown 2915, 9120 Puerto Madryn, Argentina
[g] Instituto Patagónico del Mar (IPaM), Universidad Nacional de la Patagonia San Juan Bosco, Brown 3051, 9120 Puerto Madryn, Chubut, Argentina
[h] Instituto Antártico Argentino, C1064AAF Ciudad de Buenos Aires, Argentina
[i] Centro Austral de Investigaciones Científicas (CADIC)- CONICET & Universidad Nacional de Tierra del Fuego, 9410 Ushuaia, Argentina

ARTICLE INFO

Keywords:
Climate change
Antarctic phytoplankton assemblages
Chaetoceros socialis
Shionodiscus gaarderae
Chlorophytes

ABSTRACT

The climate around the Western Antarctic Peninsula (WAP) is rapidly changing and dramatically affecting marine coastal waters. Increases in air and seawater temperatures, not matter how small, can alter coastal biological communities due to both temperature increases as well as salinity reduction from glacier melting. The aim of this study was to evaluate the individual and combined effects of elevated sea surface temperature (+4 °C) and decreased salinity (−4) on growth and assemblage composition of natural summer phytoplankton from Potter Cove (King George Island, South Shetlands, northern WAP), using an outdoor microcosm experiment. Pigment composition was analyzed by high performance liquid chromatography (HPLC/Chemtax) and species composition by light and electron microscopy. Increases in phytoplankton biomass during the first 3 days at elevated-temperatures coincided with an increase in the abundance and the specific growth rate of small centric diatoms (*Chaetoceros socialis* and *Shionodiscus gaarderae*, mostly observed in temperate waters) and unidentified small phytoflagellates < 5 μm. In contrast, pennate diatoms significantly decreased. At the end of the experiment on day 7, under nitrate and phosphate limitation, chlorophytes abundances increased under low salinity whereas prasinophytes decreased in all treatments. This study suggests that climate change could notably affect Antarctic phytoplankton composition by favouring temperate-water species previously undetected in Antarctic waters, such us *S. gaarderae*. Moreover, the observed changes in phytoplankton structure, associated with an increase of nano- over micro-size taxa, could have important implications for future Antarctic food webs.

1. Introduction

Over the last five decades, the West Antarctic Peninsula (WAP) has experienced strong atmospheric warming, with the highest heating rates recorded worldwide (Vaughan et al., 2003; Turner et al., 2005, 2014; Gutt et al., 2015). The consequent increases in air and surface seawater temperatures are responsible for the melting of glaciers that drain large amounts of freshwater and terrestrial particulate materials to coastal waters. The resulting lowering of surface seawater salinity strengthens the stratification of the water column while increased turbidity decreases light availability in surface waters (Schloss et al., 2012; Meredith et al., 2018). Since the mid-1950's, the glacial area of King George Island (KGI) in the South Shetland Archipelago (WAP) has lost 89 km^2, a 7% reduction of the total area (Simões et al., 1999). This makes KGI an ideal region for the study of climate change and its impact on marine ecosystem (Meredith et al., 2017). Planktonic organisms living in extreme environments, such as Antarctica, tend to be more sensitive to changes in environmental stressors than their temperate counterparts (Clarke et al., 2007). Because marine phytoplankton contribute ~50% to total global primary production and CO_2 fixation

* Corresponding author at: División Ficología, Facultad de Ciencias Naturales y Museo, Universidad Nacional de La Plata, 1900 La Plata, Argentina.
E-mail address: julietaantoni@hotmail.com (J.S. Antoni).

https://doi.org/10.1016/j.jembe.2020.151444
Received 10 December 2019; Received in revised form 24 June 2020; Accepted 14 August 2020
Available online 04 September 2020
0022-0981/

(Falkowski et al., 1998), they provide critical energy to the different components of the marine food web and ultimately to the top consumers (Waite et al., 1997). Therefore, it is critical to understand the responses of phytoplankton to temperature and salinity stress since variations in these abiotic factors can have profound consequences for marine food webs (Gleitz et al., 1995; Trathan et al., 2007; Lewandowska et al., 2014a) and biogeochemical cycles in the Southern Ocean (Nelson et al., 1991; Smetacek et al., 2004; Tagliabue et al., 2009).

Variations in seawater salinity and temperature have been shown to cause changes in Antarctic phytoplankton physiology under experimental conditions (Ralph et al., 2005; Hernando et al., 2015, 2018) as well as in the taxonomic structure of natural phytoplankton assemblages (Moline et al., 2001; Montes Hugo et al., 2009; Schofield et al., 2017). Previous studies demonstrated that reduced salinity, associated with meltwater input, was responsible for the increase in the relative abundance of cryptophytes (Moline et al., 2001; Garibotti et al., 2003; Mendes et al., 2013). However, little is known about the expected changes on Antarctic phytoplankton biomass and composition to the combined effect of these two stressors.

Located in KGI, Potter Cove (PC) (Fig. 1) was historically considered a low chlorophyll-a (Chl-a) area compared to other regions of the WAP, with a mean value below 1 mg Chl-a m^{-3} during 25-years (Kim et al., 2018). Previous to this study, Chemtax analyses of PC plankton samples showed a dominance of diatoms during the growing season, with a relatively low contributions of other taxonomic groups such as haptophytes and chlorophytes (van de Poll et al., 2011). More recently, anomalously large phytoplankton blooms were observed in the summer of 2010 (up to 20 mg Chl-*a* m^{-3}) and it was associated with the common large diatom species from PC, such as *Porosira glacialis* and *Thalassiosira antarctica* (Schloss et al., 2014).

After this unusual bloom, two microcosm experiments were carried out at PC in order to study the effect of decreased salinity (Hernando et al., 2015) and the combined effects of decreased salinity and increased temperature (Hernando et al., 2018) on phytoplankton stress responses, changes in assemblage composition and fatty acid profiles. These studies conducted in the summers of 2011 and 2014, respectively, exposed assemblages dominated by large diatoms (Hernando et al., 2015, 2018) to changes in these stressors. In contrast, the PC phytoplankton assemblage from the summer of 2016 used in this study was characterized by the dominance of nano-size diatoms. This is the first report of the responses of a coastal Antarctic phytoplankton assemblage dominated by small diatoms to increased temperature and decreased salinity in PC using microcosm experiments. Moreover, dominant species found at the beginning of the present experiment are mostly known to occur in subpolar waters and therefore it is relevant to analyse their potential response to increased temperature and reduced salinity conditions induced by climate change in coastal waters of the WAP. We expect their response to forecast their ability to colonize other Antarctic environments.

2. Materials and methods

2.1. Sampling site and experimental design

Microcosm experiments were conducted at the Carlini Research Station, located on the shores of PC at KGI, South Shetland Archipelago, Antarctica (62° 14′S, 58° 38′W), from January 23 to 31, 2016. The initial phytoplankton community was collected from the entrance of the cove ("outer Potter Cove" in Fig. 1) at 5 m depth with Niskin bottles. Seawater was prefiltered with a 300 μm Nitex mesh, to eliminate mesozooplankton, and used to fill 12,100-l plastic tanks, which were previously washed with 10% HCl and thoroughly rinsed with distilled water.

The experiment consisted of four treatments in triplicate (12 microcosms in total): low salinity (~30) and high temperature (+4 °C higher than ambient) (S-T+), ambient salinity (~34) and high temperature (S0T+), low salinity and ambient temperature (S-T0), and ambient salinity and temperature (S0T0, control). The values chosen for temperature increase respond to scenarios foreseen by the IPCC (2007) for sea surface temperature (see scenarios in their SPM1 table), and to a trend observed in Potter Cove from the early 1990's to 2009 (Schloss et al., 2012). Regarding the low salinity values, they are frequently observed in Potter Cove after massive glacial meltwater inflow into the coves in King George Island (Schloss, 1997; Park et al., 2020). These events are likely to be more frequent in the future (IPCC, 2019). Although by the moment of the experiment temperatures as the ones simulated in the present study had not been observed in Potter Cove, recent observations from February 2020 (Antoni, personal observation) show that such high temperatures were a realistic scenario. Therefore, temperatures 4 °C higher than the climatic anomaly were actually observed before the end of the century, as simulated in the present study. To avoid nutrient limitation during the experimental period, dissolved inorganic nutrients were added to all 4 microcosms on day 0, reaching concentrations of 8.15 ± 1.1 μmol l^{-1} NO_3, 0.81 ± 0.1 μmol l^{-1} PO_4, and 26.4 ± 4.8 μmol l^{-1} $Si(OH)_4$. No iron was added to the

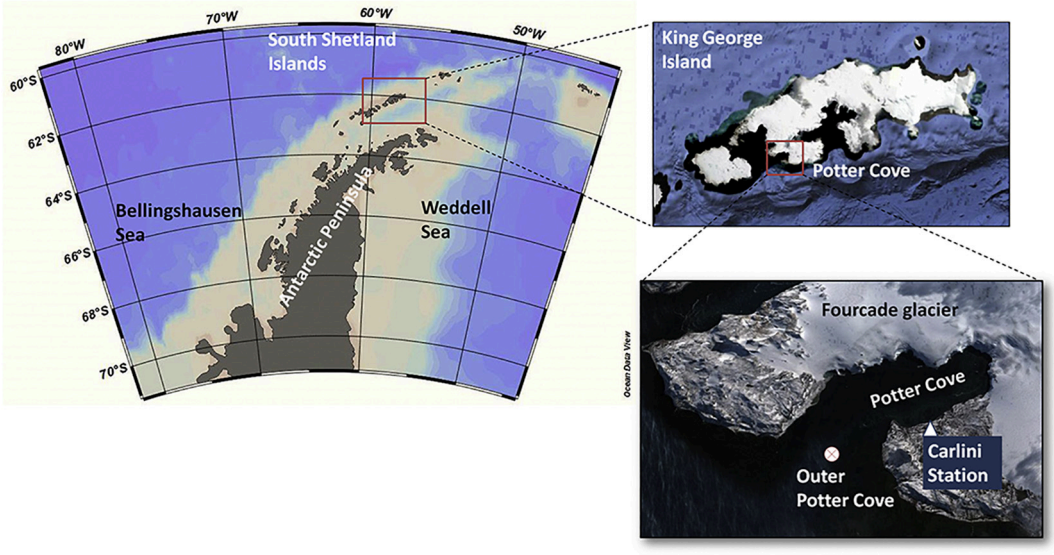

Fig. 1. Location of the sampling site in Potter Cove (62°14′S, 58°38′W), King George (25 de Mayo) Island, South Shetland Archipelago, Antarctica.

microcosms since it is not considered a limiting micronutrient in the South Shetlands coastal waters (De Jong et al., 2012). To further avoid iron contamination via dust deposition, microcosms were covered with a transparent acrylic lid, further preventing stress by UV radiation, contamination by particles and snow or rainwater during storms. An automatic mixing system was used to maintain homogeneity in the tanks and to prevent cells from settling. To avoid cell decantation, a constant agitation system was designed using a motorized stainless-steel rod coupled to a plastic propeller. Agitation, on the other hand, was gentle enough to prevent cells breakage.

For the ambient temperature treatments, the tanks were placed inside a 200-l thermal bath, connected to a stainless steel pump (Lowara, Italy) that circulated seawater extracted from coastal surface waters. For the high-temperature treatments, an automatic heating system (Recal Industry, Argentina) maintained a constant temperature increase of +4 °C with respect to ambient seawater values of ~1 °C. The heating system software allowed for temperature adjustments every 5 min. The low salinity treatments were obtained by adding 10 l of distilled water to each microcosm. To maintain constant volumes of water in all microcosms and the same cellular concentrations, the ambient salinity microcosms also received 10 l of 0.7 μm glass-fiber filtered seawater of the same salinity.

Salinity and temperature were measured in all microcosms every 12 h using a Horiba U-10 conductimeter. Salinity remained constant in all microcosms within their respective values throughout the experimental period.

2.2. Microscopic identification and quantification of phytoplankton

Samples (200 ml) from each microcosm were collected in 250 ml plastic bottles on days 0, 1, 3, 5 and 7. Water samples were treated with 4% acidic Lugol solution and kept in cold and dark conditions until analysis. Cell counts were performed by light microscopy with an inverted microscope (Leica DMIL LED phase contrast) according to the procedures described by Utermöhl (1958). Aliquots of 50 or 100 ml were allowed to settle for 24 or 48 h, respectively. At least 100 cells of the dominant taxa were counted in randomized fields at 40× and the rest of the taxa were counted in transects or in the whole camera bottom at 10–20× magnification according to their concentration and size. Phytoplankton taxa were identified to the lowest possible taxonomic level. However, some small phytoflagellates which lost their flagella during fixation were included in a single group as "unidentified phytoflagellates < 5 μm". In addition to taxonomic identification, cells of the different taxa were assigned to two groups: nano- (2–20 μm) or micro- (20–200 μm) phytoplankton.

Qualitative samples were taken with a phytoplankton net at the beginning of the experiment from the sampling location, and at the end of the experiment from each microcosm. In both cases, water samples were fixed with 4% acidic Lugol for further taxonomic identification. For diatom identification, an aliquot of each net sample was washed with distilled water several times for desalting, treated with hydrogen peroxide and heated to remove organic material following the method of Prygiel and Coste (2000). Clean diatom frustules were mounted on glass stubs, on 0.2 μm polyamide and on 2 μm polycarbonate filters, and in each case they were sputter coated with gold for scanning electron microscopy (SEM). SEM observations were performed with a JEOL JSM-6360 LV (JEOL Ltd., Tokyo, Japan) at the Universidad Nacional de La Plata and with a Gemini Zeiss DSM 982 microscope (Jena, Germany) at the Universidad de Buenos Aires. For light microscopy (LM), the clean diatom material was mounted on permanent slides using Naphrax® as in Ferrario et al. (1995). Frustules were examined with phase contrast and differential interference contrast (DIC) using two Leica DM2500 microscopes (Leica Microsystems GmbH, Wetzlar, Germany) equipped with a camera.

2.3. Pigment composition

Samples for Chl-*a* (300 ml) were collected from each microcosm on days 0, 1, 3, 5 and 7, and filtered onto 25 mm 0.7 μm (nominal porosity) glass fiber filters. Chl-*a* was extracted in 7 ml absolute methanol (Holm-Hansen and Riemann, 1978) during 24 h in cold (4 °C) and dark conditions. After the extraction period, the fluorescence of the samples were measured with a Shimadzu RF-1501 spectrofluorometer (calibrated with a pure Chl-*a* standard) and used for the calculation of Chl-*a* after correction for phaeopigments (Holm-Hansen et al., 1965).

Samples for HPLC (1000 ml) were collected from each microcosm on days 0, 5 and 7 and filtered onto 47 mm 0.7 μm (nominal porosity) glass fiber filters. Filters were flash-frozen in liquid nitrogen before storage at −80 °C until analysis at the University of Groningen, The Netherlands. Filter samples were freeze dried for 48 h prior to pigment extraction in 3 ml of 90% acetone (*v*/v) at 4 °C in the dark. Pigments were separated using a Waters 2695 HPLC system equipped with a Zorbax Eclipse XDB-C8 column (3.5 μm particle size) as described by VanHeukelem and Thomas (2001) and modified by Perl (2009). Pigments were manually identified using retention times and diode array spectroscopy (type 996, Waters, US) before quantification. Calibration of the system was performed using standards (DHI LAB PRODUCTS, Denmark) for chlorophyll c_3, peridinin, 19′-butanoyloxyfucoxanthin, fucoxanthin, neoxanthin, prasinoxanthin, 19′-hexanoyloxyfucoxanthin, alloxanthin, lutein, chlorophyll *b* and chlorophyll *a*.

CHEMTAX (v1.95) software was used to estimate the abundance of various phytoplankton groups by running 60 iterations, all having ± 35% randomized variability in the initial pigment ratios (Mackey et al., 1996). This program employs a factor analysis and steepest descent algorithm to find the best fit using known initial pigment ratios for the following six different phytoplankton classes: prasinophytes, chlorophytes, dinoflagellates, cryptophytes, haptophytes and diatoms (Wright et al., 2009, 2010; Higgins et al., 2012; Rozema et al., 2017).

2.4. Dissolved nutrients

Samples for nutrients (50 ml) were collected from each microcosm every day from 0 to 7, filtered through precombusted glass fiber filters (0.7 μm nominal porosity) and kept frozen at −20 °C for further analyses. NO_3, PO_4 and $Si(OH)_4$ concentrations were determined using a Skalar San Plus autoanalyzer (Skalar Analytical® V·B, 2005a, b, c).

2.5. Growth rates

The specific growth rates (r, d^{-1}) were measured based on cell number during the exponential phase following equation:

$$r = \frac{(\ln(Nt) - \ln(No))}{(t)}$$

where No is the initial cell density (cell $^{-1}$) and Nt is the final cell density during the exponential phase and t is the difference in time (day) between both points. This parameter was calculated for the community and most abundant taxonomic groups (> 10% of the total abundance), as well as for nano- and micro-phytoplankton size classes.

2.6. Statistical analyses

Repeated measures analyses of variance (RMANOVA, Statistica, version 9.0) were used to determine the significance of the differences in the measured parameters: phytoplankton biomass (Chl-*a*) (a), total phytoplankton abundance (b), Chl-*a* per cells (c), nitrate (d), phosphate (e), silicate (f) and HPLC pigments (g) among the four treatments (S-T+, S0T+, S-T0 and S0T0) throughout the incubation time. Changes in phytoplankton abundance through time were also evaluated with RMANOVA analysis (Statistica, version 9). The main groups and the taxa with high abundances were considered (i.e. micro-phytoplankton,

nano-phytoplankton, chlorophytes, unidentified phytoflagellates < 5, prasinophytes, centric and pennate diatoms, *Chaetoceros* spp., *Shionodiscus gaarderae*, *Pseudo-nitzschia* aff. *prolongatoides* and *Fragilariopsis cylindrus/nana*). In all cases, normality was verified using a one-sample Kolmogorov–Smirnov test ($p > 0.05$), whereas the sphericity assumption that concerns variance homogeneity was checked using the Mauchley's test. The four experimental treatments were the fixed factors and exposure time (i.e. day of incubation) was the random factor. The interaction between factors (treatment * time) was also analyzed.

The parameters (a, b, d, e and g) showed significant interactions ($p < 0.05$) and as a result, the differences between treatments at different days were analyzed using one-way ANOVA followed by Tukey test (with Bonferroni correction) (Scheiner, 2001).

For phytoplankton abundance, the interaction between factors was significant for chlorophytes, unidentified phytoflagellates < 5, prasinophytes, pennate and centric diatoms, *Chaetoceros* spp., *Shionodiscus gaarderae*, *Pseudo-nitzschia* aff. *prolongatoides* and *Fragilariopsis cylindrus/nana*. In this case, the differences between treatments at different days were statistically analyzed as was done for parameters a, b, d, e and g.

However, for micro-phytoplankton, nano-phytoplankton and total diatoms, the interaction between factors (treatment * time) was not significant ($p > 0.05$), and we used a Tukey post hoc test to evaluate the significant differences among treatments and days.

To determine differences in specific growth rate (r, d^{-1}) among the four treatments, a one-way ANOVA was used followed by Tukey test.

3. Results

3.1. Phytoplankton biomass, cell abundance and dissolved nutrients

At the beginning of the experiment (Day 0), Chl-*a* values averaged 7.8 ± 0.8 μg l^{-1} and showed no significant differences between treatments ($p = 0.16$) (Fig. 2A). In the control (S0T0) and low salinity (S-T0) treatments, Chl-*a* increased significantly until day 5 reaching a maximum value of 16.9 ± 0.8 μg l^{-1} and 17.4 ± 1.7 μg l^{-1}, respectively ($p < 0.05$) (Fig. 2A). In the S0T+ treatment, Chl-*a* increased significantly until day 3, when it reached a maximum of 28.2 ± 4.5 μg l^{-1}, doubling the values in S0T0 and S-T0 ($p < 0.05$). Finally, in S-T+ Chl-*a* increase significantly until day 3 (22.4 ± 2.3 μg l^{-1}) and remained constant from day 3 to 7 ($p < 0.05$). Both high-temperature treatments (S0T+ and S-T+) presented significantly higher Chl-*a* values with respect to the S0T0 and S-T0 on day 3 ($p < 0.05$). On day 7, Chl-*a* of the S-T+ treatment was significantly higher as compared to the other treatments ($p < 0.05$) (Fig. 2A).

Changes in total phytoplankton cell abundance differed only slightly from those for Chl-*a* (Fig. 2B). On day 0, total phytoplankton averaged 1.7 ± 0.3 × 10^6 cells l^{-1} and there were no significant differences between treatments ($p = 0.99$). In both high-temperature treatments, phytoplankton abundance increased significantly until day 3, when it reached concentrations of 8.2 ± 0.8 × 10^6 cells l^{-1} and 9.5 ± 1.3 × 10^6 cells l^{-1} for S-T+ and S0T+, respectively ($p < 0.05$). Both treatments presented significantly higher values (more than double) than those in S0T0 and S-T0 on day 3 ($p < 0.05$). In S0T0 and S-T0, abundance maxima were observed on day 5, reaching 5.8 ± 0.1 × 10^6 cells l^{-1} and 7.0 ± 0.8 × 10^6 cells l^{-1}, respectively. There were no significant differences among treatments on day 5 ($p = 0.23$) (Fig. 2B). At the end of the experiment, phytoplankton abundance decreased significantly and did not show significant differences among treatments and the S0T0 ($p < 0.05$).

The mean Chl-*a* content per cell (i.e. Chl-*a* concentration divided by total phytoplankton cell abundance) decreased in all treatments including the S0T0 until day 5 without significant differences among them ($p = 0.93$), and then increased significantly at the end of the experiment ($p < 0.05$) (Fig. 2C). On day 7, Chl-*a* per cell was significantly higher at S-T0 and S-T+ treatments with respect to the S0T0 and S0T+ ($p < 0.05$).

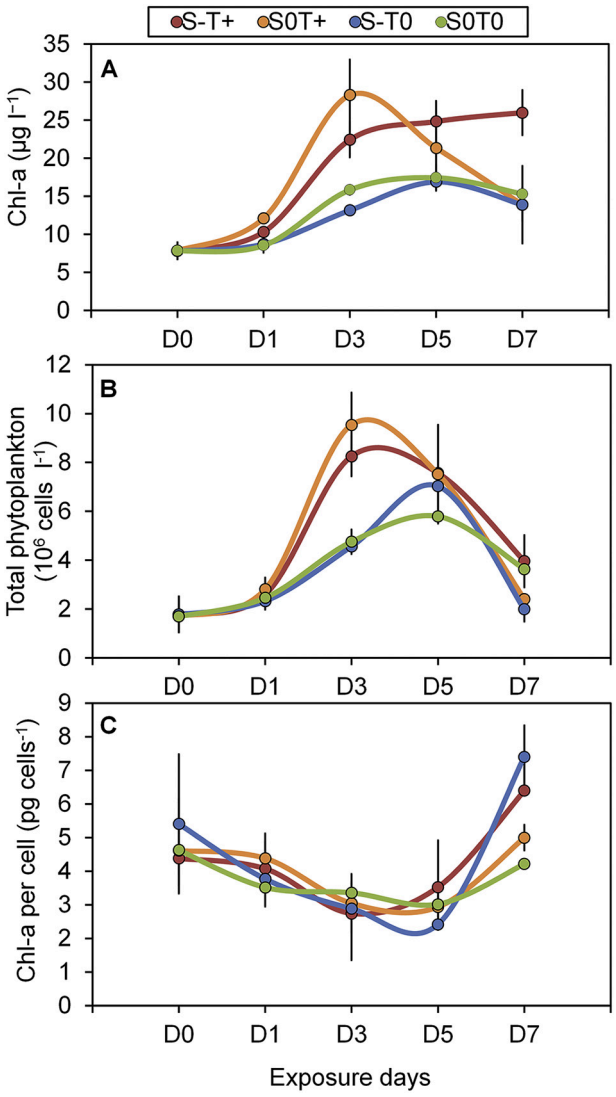

Fig. 2. Temporal evolution of (A) Chl–*a* (μg l^{-1}), (B) total phytoplankton abundance (10^6 cells l^{-1}) and (C) Chl–*a* per cell (pg $cell^{-1}$) in the experimental microcosms. S–T+ = low salinity + high temperature, S0T+ = ambient salinity + high temperature, S–T0 = low salinity + ambient temperature and S0T0 = ambient salinity and temperature. Each point represents the mean of triplicate microcosms ± SD.

Mean nutrient concentrations at day 0 in all microcosms were 8.15 ± 1.65, 0.81 ± 0.16, and 26.39 ± 4.84 μM for NO_3, PO_4 and Si $(OH)_4$, respectively (Fig. 3), without significant differences among treatments ($p = 0.99$). On day 3, the NO_3 concentration decreased significantly ($p < 0.05$) in both high temperature treatments and these values were significantly lower than those in S-T0 and S0T0 ($p < 0.05$) (Fig. 3A). On day 4 to 7, the NO_3 concentrations were below 0.3 μM and did not show significant differences among treatments ($p = 0.99$). PO_4 concentration decreased significantly at the beginning of the experiment ($p < 0.05$) and did not show differences among treatments ($p = 0.98$) (Fig. 3B). No significant differences were found for $Si(OH)_4$ concentrations among treatments ($p = 0.97$) (Fig. 3C).

3.2. Initial community composition

According to HPLC/Chemtax analyses, the initial phytoplankton

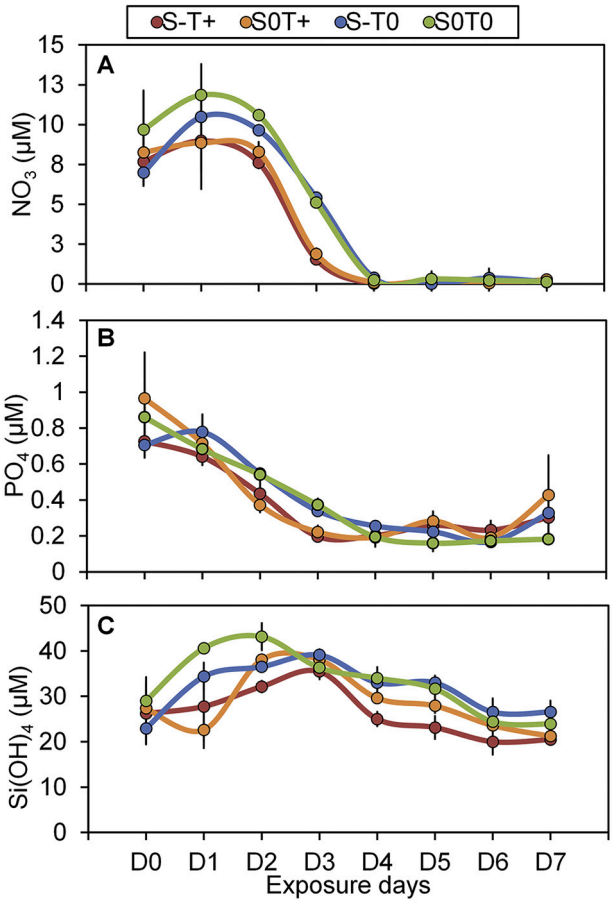

Fig. 3. Dissolved nutrient concentration of (A) NO_3 (µM), (B) PO_4 (µM) and (C) $Si(OH)_4$ (µM) in the experimental microcosms. S–T+ = low salinity + high temperature, S0T+ = ambient salinity + high temperature, S–T0 = low salinity + ambient temperature and S0T0 = ambient salinity and temperature. Each point represents the mean of triplicate microcosms ± SD.

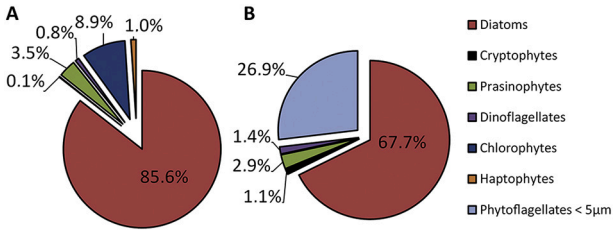

Fig. 4. Relative contribution of the different phytoplankton groups in the initial assemblage on day 0 derived from (A) HPLC and (B) microscopic analyses.

assemblage was largely dominated by diatoms that represented ≈85.6% of the total assemblage (Fig. 4A), while the other components in descending contribution were chlorophytes (8.9%), prasinophytes (3.5%), haptophytes (1.0%), dinoflagellates (0.8%) and cryptophytes (0.1%).

Microscopic analysis revealed similar results (Fig. 4B) to those obtained with HPLC, except for lower diatom relative abundance (67.7%), probably an effect of different pigment content and size of cell. The other groups and their contributions in decreasing order were: small unidentified phytoflagellates < 5 µm (26.9%), prasinophytes (2.9%), dinoflagellates (1.4%) and cryptophytes (1.1%). Based on HPLC results (Table S1 A and B), the group of small unidentified phytoflagellates < 5 µm may be composed of chlorophytes, prasinophytes and haptophytes species that could not be clearly differentiated with light microscopy.

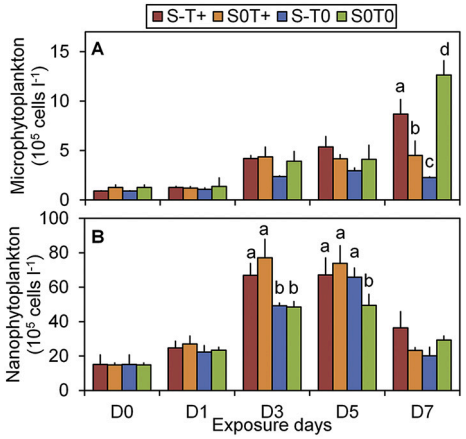

Fig. 5. Abundance estimated by microscopic analysis of (A) micro-phytoplankton (20–200 µm) and (B) nanophytoplankton (2–20 µm). S–T+ = low salinity + high temperature, S0T+ = ambient salinity + high temperature, S–T0 = low salinity + ambient temperature and S0T0 = ambient salinity and temperature. Each bar represents the mean of triplicate microcosms ± SD. Significant (Tukey Test) differences between treatments on the same day are denoted with different letters for $p < 0.05$.

3.3. Temporal evolution of the main phytoplankton groups

The initial (day 0) relative abundance of micro-phytoplankton represented ≈4–25% of total phytoplankton (data not shown), with an average abundance of 1.1 ± 0.2 × 10^5 cells l^{-1} (Fig. 5A). In high-temperature treatments and S0T0, the abundance increased significantly towards day 7, with maximum values of 7.3 ± 3.5 × 10^5 cells l^{-1} (S-T+), 4.5 ± 1.4 × 10^5 cells l^{-1} (S0T+) and 12.6 ± 1.4 × 10^5 cells l^{-1} (S0T0). In contrast, the maximum abundance in S-T0 was observed on day 5, reaching 2.9 ± 0.2 × 10^5 cells l^{-1}. On day 7, micro-phytoplankton abundance in S0T0 was significantly higher compared to all treatments, and that observed in the S-T0 was significantly lower than in high-temperature treatments.

On day 0, the relative abundance of nano-phytoplankton represented ≈75–86% of total phytoplankton, with an average abundance of 14.9 ± 0.1 × 10^5 cells l^{-1} (Fig. 5B). In high-temperature treatments, the abundance increased significantly by day 3 with maximum values of 67 ± 7 × 10^5 cells l^{-1} (S-T+) and 77 ± 11 × 10^5 cells l^{-1} (S0T+). These values were significantly higher compared to S0T0 and S-T0 ($p < 0.05$). In the S0T0 and S-T0, maximum abundances were observed on day 5, reaching 49 ± 6 × 10^5 and 65 ± 5 × 10^5 cells l^{-1} respectively. On day 7, nano-phytoplankton abundance decreased significantly in all treatments and S0T0 ($p < 0.05$).

3.3.1. Chlorophytes

On day 0, the relative abundance of chlorophytes estimated by HPLC analysis represented ≈8.8–9.0% of total phytoplankton in all treatments. No significant changes were observed at day 5 among treatments ($p = 0.56$) (Fig. 6). On day 7, there was a significant increase in their relative abundance under low salinity conditions (S-T0), with a range of ≈8.8–11% ($p < 0.05$).

3.3.2. Unidentified small phytoflagellates

The relative contribution of unidentified phytoflagellates (< 5 µm) to total phytoplankton cell abundance ranged from ≈20 to 40% throughout the experiment. On day 0, the abundance of unidentified phytoflagellates (< 5 µm) estimated by microscopy averaged 0.4 ± 0.1 × 10^6 cells l^{-1} in all treatments (Fig. 7A). In the high-temperature treatments, they increased significantly until day 3 with a maximum abundance of 2.2 ± 0.5 × 10^6 cells l^{-1} (S0T+) and 1.7 ± 0.4 × 10^6 cells l^{-1} (S-T+) ($p < 0.05$), and their abundances

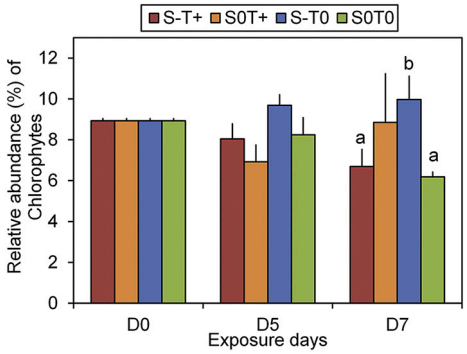

Fig. 6. Relative abundance (%) of chlorophytes based on HPLC data. S–T+ = low salinity + high temperature, S0T+ = ambient salinity + high temperature, S–T0 = low salinity + ambient temperature and S0T0 = ambient salinity and temperature. Each bar represents the mean of triplicate microcosms ± SD. Significant (Tukey Test) differences between treatments on the same day are denoted with different letters for $p < 0.05$.

were significantly higher compared to S0T0 and S-T0. In the S0T0 and S-T0, maximum abundances were observed on day 5, reaching $1.2 \pm 0.1 \times 10^6$ and $1.6 \pm 0.4 \times 10^6$ cells l^{-1} respectively. After these maximum values, abundances decreased significantly in all treatments until the end of the experiment ($p < 0.05$).

3.3.3. Prasinophytes

The relative contribution of prasinophytes to total phytoplankton estimated by microscopy and HPLC analyses ranged from ≈0.05–2.74 and 1.35–3.53% respectively throughout the experiment. On day 0, the abundance of prasinophytes averaged $0.055 \pm 0.003 \times 10^6$ cells l^{-1} and showed no significant differences between treatments ($p = 0.99$). In the high-temperature treatments, the maximum values were observed on day 3, reaching $0.07 \pm 0.03 \times 10^6$ cells l^{-1} (S0T+) and $0.12 \pm 0.02 \times 10^6$ cells l^{-1} (S-T+) (Fig. 7B). In S-T0, a maximum of $0.10 \pm 0.04 \times 10^6$ cells l^{-1} was observed on day 5. Until the last day of the experiment, their abundance remained constant at S0T0 ($0.06 \pm 0.01 \times 10^6$ cells l^{-1}) but decreased significantly in all other treatments on day 7, reaching values close to 0 ($p < 0.05$).

3.3.4. Diatoms

The relative contribution of diatoms to total phytoplankton estimated by microscopy and HPLC analyses ranged from ≈49–84 and 85–92% respectively throughout the experiment but showed no significant differences between treatments ($p = 0.36$) (Table S2). By contrast, differences were evident when diatoms were classified according to their symmetry (i.e. pennate vs. centric) and species composition (see next section).

The abundance of total diatoms (both centric and pennate diatoms) from microscopic analysis averaged $1.3 \pm 0.4 \times 10^6$ cells l^{-1} in all treatments on day 0 (Fig. S1). In the high-temperature treatments, diatoms presented a maximum on day 5 with an abundance of $6.5 \pm 0.8 \times 10^6$ cells l^{-1} (S0T+) and $5.5 \pm 0.7 \times 10^6$ cells l^{-1} (S-T+). The maximum abundances in S0T0 and S-T0 were observed on day 5, reaching $4.5 \pm 0.6 \times 10^6$ cells l^{-1} and $5.1 \pm 0.3 \times 10^6$ cells l^{-1}, respectively. After these maxima, the abundance of diatoms decreased significantly in all treatments ($p < 0.05$).

Centric diatoms represented ≈45–57% of total phytoplankton and the ≈83–84% of the total diatoms at day 0 (data not shown), with an initial average abundance of $0.9 \pm 0.1 \times 10^6$ cells l^{-1}. In high-temperature treatments, abundances increased significantly towards day 5, with a maximum abundance of $5.7 \pm 0.7 \times 10^6$ cells l^{-1} (S0T+) and $4.6 \pm 0.6 \times 10^6$ cells l^{-1} (S-T+), that were significantly higher than in S0T0 and S-T0 on days 3 and 5. In S0T0 and S-T0, the maximum values were observed on day 5 with an abundance of $2.8 \pm 0.5 \times 10^6$ cells l^{-1} and $3.5 \pm 0.3 \times 10^6$ cells l^{-1} respectively. From day 5 to 7, their abundance remained constant in S0T0, but decreased significantly in all other treatments ($p < 0.05$), and showed significant differences between all treatments and S0T0 ($p < 0.05$) (Fig. 7C). Centric diatoms were mostly represented by *Chaetoceros socialis* (Fig. 9 A-D) and other small sized (< 20 μm) solitary unidentified specimens of *Chaetoceros*, followed by *Shionodiscus gaarderae* (Fig. 9E), *Porosira glacialis* (Fig. 9F), *Thalassiosira antarctica* (Fig. 9G) and other less abundant species from the microplankton such as *Odontella weisfloggi*, *Minidiscus chilensis*, *Eucampia antarctica* and *Actinocyclus actinochilus*.

On day 0, the genus *Chaetoceros* represented ≈65–68% of total centric diatoms and ≈28–44% of total phytoplankton (data not shown), with an initial average abundance of $0.62 \pm 0.16 \times 10^6$ cells l^{-1} (Fig. 8A). In high-temperature treatments and S0T0 they increased significantly by day 3 with a maximum abundance of $3.5 \pm 0.6 \times 10^6$ cells l^{-1} (S0T+), $2.8 \pm 0.1 \times 10^6$ cells l^{-1} (S-T+) and $2.1 \pm 0.1 \times 10^6$ cells l^{-1} (S0T0), with significantly higher abundances at both high-temperature treatments than in S0T0 and S-T0 ($p < 0.05$) (Fig. 8A). In contrast, the maximum abundance in S-T0 was observed on day 5, reaching $2.4 \pm 0.4 \times 10^6$ cells l^{-1}. After their maxima, *Chaetoceros* abundance decreased significantly in all treatments ($p < 0.05$) (Fig. 8A).

The next most abundant diatom species, *S. gaarderae,* represented

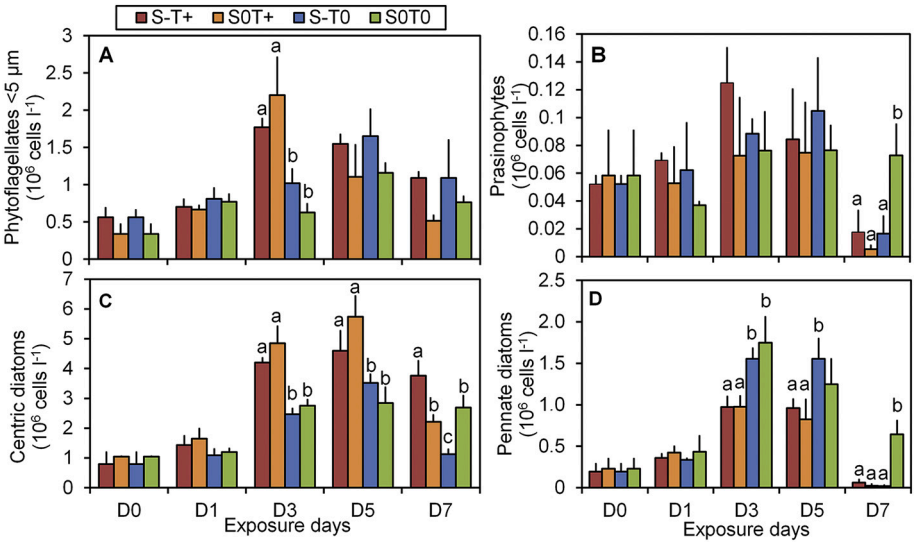

Fig. 7. Abundance estimated by microscopic analysis of (A) unidentified phytoflagellates (< 5 μm), (B) prasinophytes, (C) centric diatoms and (D) pennate diatoms. S–T+ = low salinity + high temperature, S0T+ = ambient salinity + high temperature, S–T0 = low salinity + ambient temperature and S0T0 = ambient salinity and temperature. Each bar represents the mean of triplicate microcosms ± SD. Significant (Tukey Test) differences between treatments on the same day are denoted with different letters for $p < 0.05$.

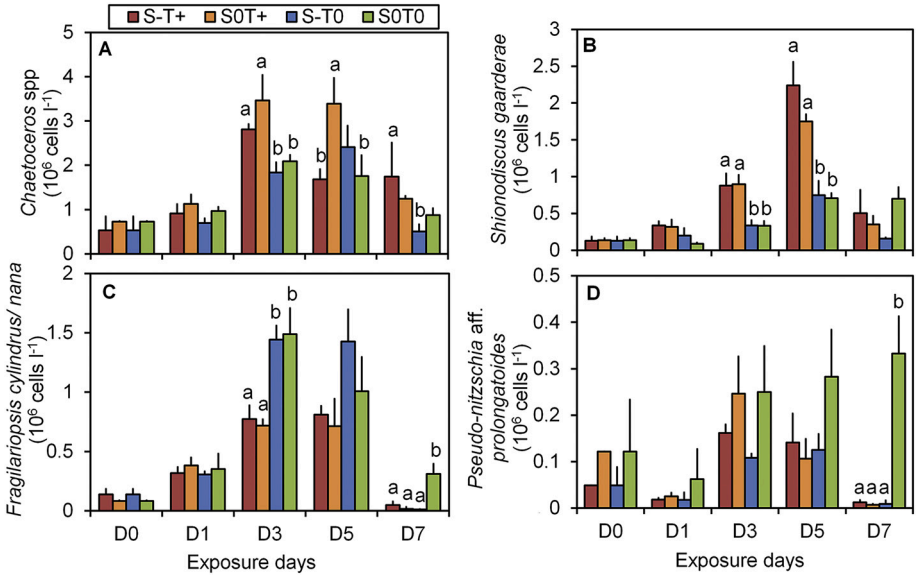

Fig. 8. Abundance of (A) *Chaetoceros* spp., (B) *Shionodiscus gaarderae,* (C) *F. cylindrus/nana* and (D) *P.* aff. *prolongatoides* with respect to total phytoplankton, estimated by microscopic analysis. S–T + = low salinity + high temperature, S0T + = ambient salinity + high temperature, S–T0 = low salinity + ambient temperature and S0T0 = ambient salinity and temperature. Each bar represents the mean of triplicate microcosms ± SD. Significant (Tukey Test) differences between treatments on the same day are denoted with different letters for $p < 0.05$.

≈8–9% of total phytoplankton throughout the experiment and its average abundance on day 0 was 0.13 ± 0.04 × 10^6 cells l^{-1} (Fig. 8B). In high-temperature treatments, abundances increased significantly towards day 5, with a maximum abundance of 1.7 ± 0.1 × 10^6 cells l^{-1} (S0T+) and 2.2 ± 0.3 × 10^6 cells l^{-1} (S-T+), that were significantly higher than in S0T0 and S-T0 on days 3 and 5. In S0T0 and S-T0, the maximum values were observed on day 5 with an abundance of 0.7 ± 0.1 × 10^6 cells l^{-1} and 0.8 ± 0.2 × 10^6 cells l^{-1} respectively. From days 5 to 7, their abundances remained constant at S0T0 but decreased significantly in all other treatments ($p < 0.05$).

Pennate diatoms represented ≈8–9% of total phytoplankton and the ≈15–16% of the total diatoms at day 0 (data not shown). The abundance of pennate diatoms increased significantly in all treatments towards day 3 ($p < 0.05$) (Fig. 7D), with maximum values of 1.7 ± 0.3 × 10^6 cells l^{-1} (S0T0) and 1.5 ± 0.1 × 10^6 cells l^{-1} (S-T0), which were significantly higher than those observed in the high-temperature treatments. These differences remained on day 5, while from day 5 to 7, pennate diatom abundance decreased significantly in all treatments ($p < 0.05$). However, in S0T0 the abundance of pennate diatoms decreased more gradually in comparison to S-T+, S0T+ and S-T0, which showed significantly lower values at day 7 ($p < 0.05$) (Fig. 7D). Pennate diatoms were mostly represented by the small species *Fragilariopsis cylindrus/nana* (< 10 μm) (Fig. 9H), which accounted for 61% of total pennate diatoms throughout the experiment, followed by *Pseudo-nitzschia* aff. *prolongatoides* (35%) (Fig. 9I). Other species observed in minor relative abundance (< 2%), included other *Pseudo-nitzschia* (mainly represented by *Pseudo-nitzschia* sp. as shown in Fig. 9J) and *Fragilariopsis* species (> 15 μm), such as *F. curta*, *F. obliquecostata,* and *F. ritscheri*, as well as *Cocconeis* spp., *Navicula perminuta*, *Licmophora belgicae*, and *Pseudogomphonema kamchaticum*.

The abundance of *F. cylindrus/nana* increased significantly until day 3 in S0T0 and S-T0 ($p < 0.05$) (Fig. 8C), with maximum values of 1.5 ± 0.2 × 10^6 cells l^{-1} and 1.4 ± 0.1 × 10^6 cells l^{-1} respectively, which were significantly higher than those observed in the high-temperature treatments ($p < 0.05$). In the high-temperature treatments, their abundance increased significantly until day 5 ($p < 0.05$), with an abundance of 0.7 ± 0.2 × 10^6 cells l^{-1} (S0T+) and 0.8 ± 0.1 × 10^6 cells l^{-1} (S-T+). On day 7, the abundance decreased significantly in all treatments, and showed significantly higher values in S0T0 than in the others treatments ($p < 0.05$).

The contribution of *P.* aff. *prolongatoides* to total phytoplankton was lower than 5% throughout the experiment and showed no significant differences among treatments until day 5 ($p = 0.99$). On day 7, its abundance decreased significantly in all treatments but increased in S0T0 ($p < 0.05$) (Fig. 8D).

3.3.5. Other minor phytoplankton groups

Throughout the experiment, in both HPLC and microscopic analyses, there were no significant differences in the abundances of cryptophytes, dinoflagellates (mostly represented by the nanoplanktonic species *Prorocentrum* aff. *balticum* and *Katodinium* aff. *glaucum*) (Fig. S2), and haptophytes ($p = 0.95$). These groups represented less than 1% of total phytoplankton throughout the experiment. In general, microzooplankton were extremely scarce, mostly represented by heterotrophic dinoflagellates and small ciliates; mesozooplankton were absent, which indicates that they were effectively removed with the 300 μm net when filling the tanks.

3.4. Specific growth rate of the community and main phytoplankton groups

Phytoplankton community growth rate was significantly higher in the high temperature treatments compared with S0T0 and S-T0 ($p < 0.05$) (Fig. 10A). Microphytoplankton specific growth rate did not show significant differences between treatments ($p = 0.76$). By contrast, nanophytoplankton growth rates in both high-temperature treatments (S0T+ and S-T+) were significantly higher than in S-T0 and S0T0 ($p < 0.05$) (Fig. 10A).

In regards to the main taxonomic groups, unidentified phytoflagellates < 5 μm and centric diatoms both showed significantly higher growth rates in S0T+ than in S0T0 and S-T0 ($p < 0.05$) (Fig. 10B). In contrast, pennate diatoms showed significantly lower values in S0T+ treatment than in S-T0 and S0T0 ($p < 0.05$).

The genus *Chaetoceros* and *Shionodiscus* showed similar responses, with significantly higher growth rates in both high-temperature treatments ($p < 0.05$) (Fig. 10C). In contrast, *F. nana/cylindrus* growth rates for S-T+ and S0T+ were significantly lower than those for S-T0 and S0T0 ($p < 0.05$), whereas no significant differences in growth rates were observed for *P.* aff. *prolongatoides* among treatments ($p = 0.79$).

4. Discussion

Abrupt temperature changes such as heatwaves and such as those simulated in the present study have doubled in frequency and have become longer-lasting, more intense and more extensive (IPCC, 2019).

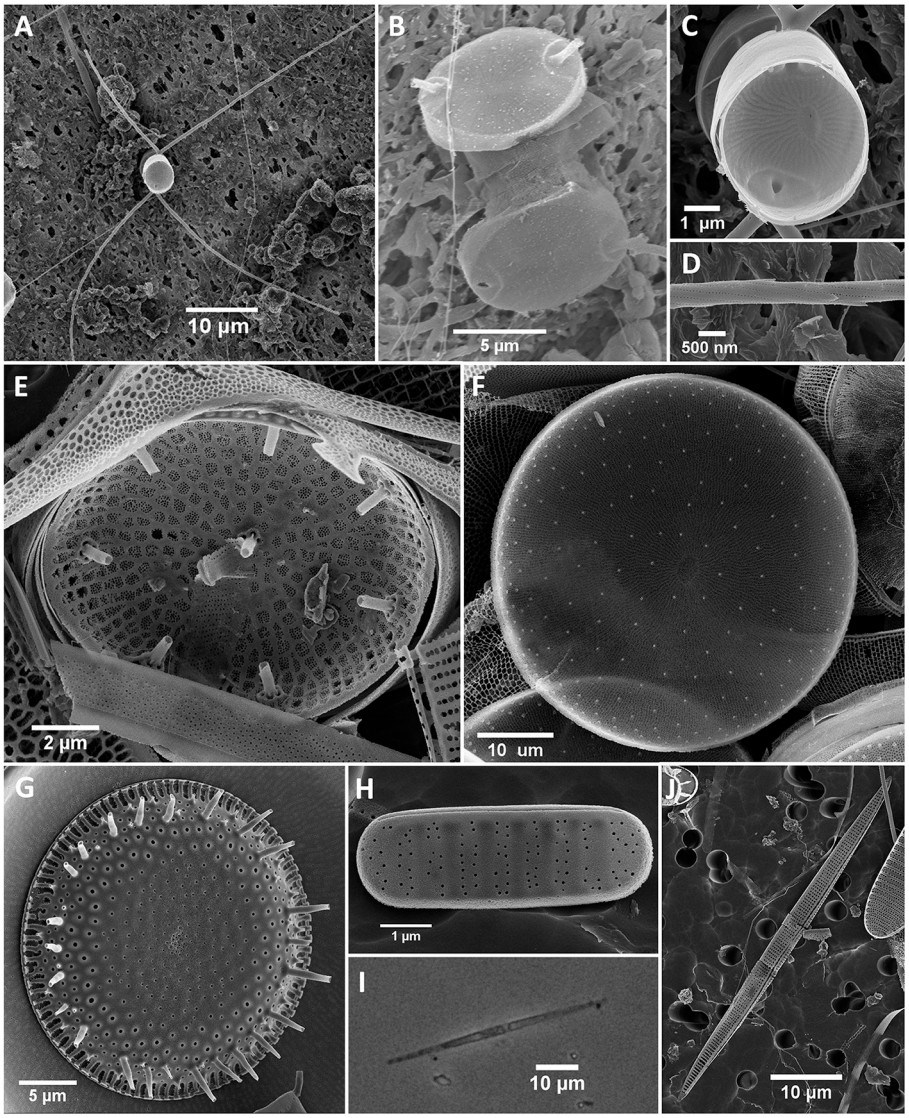

Fig. 9. EM micrographs of diatom species observed in the experiment. (A–D) *Chaetoceros socialis*; E) *Shionodiscus gaarderae;* F) *Porosira glacialis*; G) *Thalassiosira scotia*; H) *Fragilariopsis cylindrus/nana*; I) *Pseudo–nitzschia* aff. *prolongatoides* (LM) and J) *Pseudo–nitzschia* sp.

Moreover, there are very likely (i.e., there is very high confidence) for these events to further happen in the future (IPCC, 2019). Natural communities in these short-term warming scenarios will probably not have the time to acclimate to higher temperatures, a process that needs over 6–7 days (Gao et al., 2017). Given the current changes in Antarctic environments (Convey et al., 2009; Turner et al., 2014; Chown et al., 2015), it is important to consider both the responses of phytoplankton assemblages and of individual species to environmental stressors because of their impacts on marine food webs. At both population and community levels, phytoplankton use different strategies in response to environmental stress, such as changes in the composition of the assemblages (Alves-de-Souza et al., 2008), growth rates (Berges et al., 2002), morphological and physiological characteristics at the cellular level, and enzymatic activity (Arrigo and Sullivan, 1992; Gao et al., 2000; Petrou et al., 2011). In this study, we evaluated the effects of seawater salinity and temperature on Antarctic phytoplankton species composition and growth rates, and showed that phytoplankton taxonomic groups respond differently to variations in these stressors.

In previous microcosm studies in PC during 2011 and 2014, the initial phytoplankton assemblages were characterized by high numbers of micro-sized (> 20 µm) diatoms such as *Porosira glacialis*, *Thalassiosira antarctica* and *Odontella weissflogii* (Hernando et al., 2015, 2018). The dominance of these micro-sized diatoms during summer blooms was recurrently observed in PC and surrounding areas of King George Island since 1991 (Schloss and Ferreyra, 2002; Schloss et al., 2014; Lange et al., 2007; Kopczyńska, 2008). In contrast, in our 2016 experiment, the initial phytoplankton assemblage was dominated by nano-size (< 20 µm) diatoms such as species from the genera *Chaetoceros* and *Shionodiscus*. The initial composition of the phytoplankton assemblage as well as total biomass are the result of the interaction of a series of environmental conditions (see Schloss et al., 2014). It should be noted, however, that summer sea surface temperature was significantly higher and salinity significantly lower than in the previous year ($p < 0.05$ for both variables as contrasted to 2015 by means of a Kruskal–Wallis one-way analysis of variance), therefore explaining in part the presence of the described assemblage. Blooms of nano-size species such as small *Chaetoceros* are rarely observed in open or coastal waters of Antarctica (McMinn and Hodgson, 1993; Moisan and Fryxell, 1993; Kang et al., 2001; Kopczyńska, 2008). Therefore, this 2016 study provides a new look at the effect of salinity and temperature on Antarctic coastal phytoplankton due to the exposure of an ambient phytoplankton assemblage which composition was radically different from that present in previous studies (Hernando et al., 2015, 2018). Moreover, initial Chl-*a* levels were 8 µg l^{-1} (Fig. 2A), which are markedly

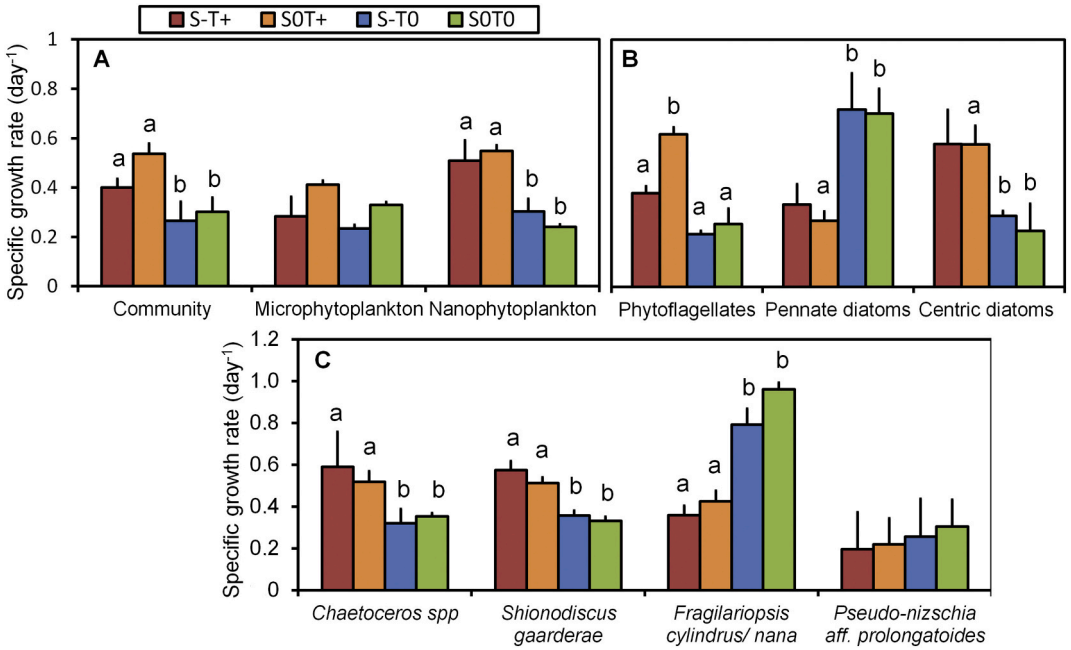

Fig. 10. Specific growth rate (r, day^{-1}) of (A) community, microphytoplankton and nanophytoplankton, (B) Phytoflagellates, pennate diatoms and centric diatoms, (C) *Chaetoceros* spp., *Shionodiscus gaarderae*, *P.* aff. *prolongatoides* and *F. cylindrus/nana*. S–T+ = low salinity + high temperature, S0T+ = ambient salinity + high temperature, S–T0 = low salinity + ambient temperature and S0T0 = ambient salinity and temperature. Each bar represents the mean of triplicate microcosms ± SD. Significant (Tukey Test) differences between treatments on the same day are denoted with different letters for $p < 0.05$.

higher than those observed in the previous experiments by Hernando et al. (2015, 2018), and historically they are exceptionally high for this location during summer blooms (Schloss, 1997). Because of the high initial biomass, nutrients were added at the beginning of the experiment in all microcosms with the intention of avoiding nutrient exhaustion throughout the course of the experiment. However, the exceptionally high initial phytoplankton biomass led to unexpected NO_3 and PO_4 drawdown and exhaustion by day 4 (Fig. 3A, B), but without significant differences among treatments, and thus equally affecting phytoplankton assemblages. Consequently, we assume phytoplankton composition changes observed after day 4 are the result of the experimental salinity and temperature treatments, under the exhaustion of NO_3 and PO_4.

4.1. Effects of increased temperature

Under elevated temperatures, phytoplankton biomass (Fig. 2A), cell abundances (Fig. 2B), and the specific growth rate (Fig. 10A) increased two-fold in comparison to those in control conditions (S0T0) by day 3. Early studies (e.g. Neori, 1982) already indicated that Antarctic phytoplankton achieve their maximum growth rate at a few degrees higher than ambient temperatures, and that both photosynthesis and growth rate decreased exponentially at above 7 °C. Despite the increase in seawater temperature in PC in the last 20 years (Schloss et al., 2012), water temperature is still less than that 7 °C threshold. But more importantly, this responses cannot be generalized as different species respond differently to an increase in seawater temperature (Eppley, 1972; Berges et al., 2002; Kremp et al., 2012), mostly associated with cell biochemistry (Gao et al., 2000; Teoh et al., 2004).

In the present study, centric diatoms, mainly represented by small species such as *Chaetoceros socialis* and *Shionodiscus gaarderae*, increased their abundance (Fig. 8A, B) and specific growth rate (Fig. 10C) in response to enhanced temperature. Until recently, *C. socialis* was considered a cosmopolitan species (Ostenfeld, 1913; Rines and Hargraves, 1988), particularly common in Arctic and Antarctic marine waters, where it forms extensive blooms (Booth et al., 2002; Kopczyńska, 2008). However, a detailed molecular and morphological examination of *C. socialis* strains from different parts of the world (excluding Antarctica) indicated the presence of two main clades or species (Chamnansinp et al., 2013), one from cold waters (*C. gelidus* sp. nov.) and the other one from warmer waters (*C. socialis*). Surprisingly, the specimens observed in our study corresponded to the species *C. socialis* (sensu Chamnansinp et al., 2013), characterized by setae extending from the valve at some distance from the margin and all setae covered by spines (Fig. 9A-D). Further molecular analyses are needed to confirm their identity, yet our results suggest that warm-waters *C. socialis* sensu Chamnansinp et al. (2013) can be favoured by temperature increases in Antarctic waters.

Alverson et al. (2006) transferred several *Thalassiosira* species to a new genus called *Shionodiscus*, which is characterized by the labiate process placed on the valve face, a strutted process with longer extensions inwards and reduced or absent outward extensions. Several small *Shionodiscus* species are known to occur in Antarctic waters, such as *S. gracilis*, *S. gracilis* var. *expecta*, *S. perpusilla*, *S. oestrupii*, *S. frenguelli*, *S. frenguelliopsis*, *S. poroseriata*, *S. ritscheri*, and *S. trifulta* (Scott and Marchant, 2005, all of them previously described as *Thalassiosira* species). However, the valve morphology of the specimens observed in our study does not coincide with any of these species, but corresponds to *S. gaarderae* described by Ferrario et al. (2018). This small species is known to occur in the Norwegian and North Seas, with peak abundance (5×10^5 cells l^{-1}) during spring in sea water temperature ~ 9 °C, and also in sub-Antarctic waters from the Argentine Sea (Ferrario et al., 2018). In the latter, extensive blooms of *S. gaarderae* (up to 4.5×10^6 cells l^{-1}) were recorded during spring in shelf-break waters from 39°S to 48°S at temperatures ranging from 5 to 9 °C (Ferrario et al., 2018). In our experiments, *S. gaarderae* continued to grow in high-temperature treatments until day 5, when NO_3 concentrations were on average 0.2 μM (Fig. 3A), and thus theoretically limiting phytoplankton growth (Ogilvie et al., 2003; Carter et al., 2005; Millero, 2016). As it is known, diatoms have the ability to store nitrogen when available, to use it for growth during periods when it is limiting (Lomas and Glibert, 2000). This strategy, in addition to its preference for warmer temperatures, could allow *S. gaarderae* to outcompete native diatoms species under high temperature/low nutrient conditions, thus changing the

composition of the phytoplankton assemblage. To the best of our knowledge, our study is the first to find *S. gaarderae* in Antarctic waters and to show an association between elevated temperatures (4 °C above ambient) and the high abundance of the genus *Shionodiscus* in Antarctic waters.

In contrast to the increase in the abundance of some centric diatoms, the abundance of pennate diatoms such as *F. cylindrus/nana* and *P.* aff. *prolongatoides* significantly decreased (Fig. 8C, D) (and the specific growth rate of *F. cylindrus/nana* showed in Fig. 10C) under enhanced temperatures during this study. Both *Fragilariopsis* species are considered endemic to polar and subpolar regions in the Arctic and the Antarctic (Lundholm and Hasle, 2008), and are common members of summer diatom blooms (Scott et al., 1994; Fiala et al., 2006; Kopczyńska, 2008; Lundholm and Hasle, 2008; Cefarelli et al., 2010). Particularly, *F. cylindrus* is known to dominate within brine channels and pockets in polar sea ice (Günther and Dieckmann, 2001; Lizotte, 2001), where temperatures can reach values as low as −20 °C (Maykut, 1986; Eicken, 1992). This adaptation to extremely low temperatures has been related to the presence of a multigene family of antifreeze proteins (Baardsnes et al., 2001). Instead, *P. prolongatoides* has been described as endemic to Antarctica (Hasle and Syvertsen, 1997), and was observed to bloom (i.e. 7.2×10^5 cells l^{-1}) in the Southern Weddell Sea during summer at 0.31 °C and salinity of 33.59 (Almandoz et al., 2008). The fact that natural populations of these pennate diatoms seem to be better adapted to cold temperatures could explain the observed negative response under high temperature treatments.

Unidentified phytoflagellates < 5 μm increased their abundance and specific growth rate in response to enhanced temperature (Fig. 7A). This trend towards an increase of smaller flagellates under elevated temperature conditions has been previously reported in experimental studies with Antarctic marine species, such as *Phaeocystis antarctica* that showed optimum growth at temperatures around 4 to 5 °C (Wang et al., 2010; Zhu et al., 2017).

In addition to the observed changes in the taxonomic composition of phytoplankton assemblage, higher temperature also resulted in overall changes in the size structure of phytoplankton assemblages, with an increase of nano- over micro-sized diatoms throughout the experiment (Fig. 5). This trend towards a dominance of smaller taxa under warmer conditions has been previously reported for both marine and freshwater environments (Atkinson et al., 2003; Daufresne et al., 2009; Li et al., 2009; Finkel et al., 2010).

Many experimental studies support the hypothesis that smaller plankton species have a greater competitive advantage than larger species at higher temperatures (e.g. Hare et al., 2007; Morán et al., 2010; Peter and Sommer, 2012; Coello-Camba et al., 2015; Ward, 2015). Likewise, a global data set on size-fractionated chlorophyll distributions collected in the open ocean, suggest that the relative contribution of small cells in the community increases with increasing temperature, regardless of ambient nutrient availability (Mousing et al., 2014). This is an adaptive advantage to enhanced temperatures, and especially when nutrients concentrations decrease, as small cells have a lower minimum metabolic requirement that selectively allows them to survive at much lower resource concentrations than larger cells (Shuter, 1978; Grover, 1991). Regarding nutrients consumption, lower half-saturation constants due to the higher surface area to volume (SA/V) ratios and higher rates of nutrient uptake per unit biomass (e.g. Eppley and Thomas, 1969; Aksnes and Egge, 1991; Hein and Pedersen, 1995; Irwin et al., 2006) characterize small as compared to big phytoplankton cells. Our results agree with these observations, in the sense that the smaller cells size was found along with low nutrients concentrations. This would also point towards the idea that it is not a single factor that can held responsible for the decrease in size in phytoplankton under high temperatures (Marañón et al., 2012; Lewandowska et al., 2014b).

A similar trend has been observed in zooplankton communities with a replacement of larger species by smaller ones under higher temperatures (Brucet et al., 2010); however, this finding is not universally accepted (Gardner et al., 2011; Rüger and Sommer, 2012). These changes in the structure of plankton communities could affect higher levels in the trophic food web because the herbivory of heterotrophic organisms is directly related to the abundance and size of their prey (Frost, 1972; Cohen et al., 2003).

The combined effects of temperature and nutrients have been studied in other environments (Skau et al., 2017). Our experimental design does not allow distinguishing between the effects of temperature increase and nutrients decrease. This would require a factorial experiment to specifically address this question, which is something that should be considered in future works.

4.2. Effects of reduced salinity

We found no significant changes in phytoplankton biomass (i.e. Chl-*a*) and total abundance in the low salinity treatments when compared to the S0T0, except on day 3, when there was a small decrease under S-T0 (Fig. 2A, B). These results are similar to the previous findings of Hernando et al. (2018) but contrast with Hernando et al. (2015), where Chl-*a* and cell abundance showed a significant decrease at low salinity conditions (Fig. 2C).

In contrast to the lack of significant changes in Chl-*a* and total abundance under lower salinity, we measured significant changes in the composition of the phytoplankton assemblages. The relative abundance of chlorophytes increased in the low salinity treatment on day 5 (Fig. 6). As far as we know, this is the first experimental study from Antarctic waters evidencing an increase of small chlorophytes under low salinity. Unicellular chlorophytes are not well known and usually represent a minor component of Antarctic marine phytoplankton assemblages (Moline and Prézelin, 1996; Ishikawa et al., 2002; Lee et al., 2016). Previous studies evaluated the growth of two marine chlorophyte species under salinity stress. *Chlamydomonas* sp. from the Arctic was more tolerant to reduced salinity (< 33) rather than elevated salinity (Søgaard et al., 2011). In contrast, *Dunaliella tertiolecta* continued to grow under hypotonic stress with no signs of physical damage (Gilmour et al., 1984). As for field samples in other areas, we found that chlorophytes are associated with low salinity waters (Tragin and Vaulot, 2018).

In contrast to the positive response of chlorophytes, the relative abundance of small centric diatoms of the genus *Shionodiscus* and the pennate diatoms *P.* aff. *prolongatoides* and *F. cylindrus/nana* decreased at the end of the experiment under reduced salinity (Fig. 8). Hernando et al. (2015) found that small pennate diatom assemblages mainly represented by *F. cylindrus/nana*, *Navicula glaciei*, *N. perminuta* and *Nitzschia* cf. *lecointei* significantly increased their abundance under low salinity at the end of the experiment (days 6 and 8), for which the initial phytoplankton assemblage composition was characterized by large centric diatoms. However, despite this apparent difference between the studies about the abundance of *F. cylindrus/nana,* it should be noted that in our study they also significantly increased on day 5, compared to the S0T0, but then decreased at the end of the experiment (day 7). Another study also showed that *F. cylindrus* has a high tolerance to osmotic stress, due to the presence of genes that allow adaptation to low salinity conditions in polar environments (Mock et al., 2006).

4.3. Combined effects of increased temperature and reduced salinity

When phytoplankton assemblages were exposed to the combined stressors (S-T+), Chl-*a* significantly increased and achieved the highest values at the end of the experiment (Fig. 2A). In contrast, total phytoplankton abundance and composition did not show significant changes over time. Both results point to an increase in the concentration of Chl-*a* per cell. In fact, both low-salinity treatments (S-T0 and S-T+) showed significantly higher (almost double) Chl-*a* per cell than in S0T0 and S0T+ (Fig. 2C). Changes in the Chl-*a* concentration per cell have been previously observed as a consequence of osmotic stress on other species

(García Valenzuela et al., 2005). Particularly, some marine microalgae species such as *Porphyridium* sp., *Amphidinium carleri* and *Olisthodiscus* sp. produced higher quantity of Chl-*a* per cell in optimal salinity conditions in culture, and this response was independent of growth rate (McLachlan, 1961). The high Chl-*a* value in the S-T+ contrasted with the S-T0 treatment on day 7, which could have been related to the combined effect of temperature and salinity. Higher temperature probably stimulated cell division of those species more able to grow under high temperature, causing the increasing of total cell number, whereas the salinity effect additionally increased the Chl-*a* per cell (McLachlan, 1961), leading to the observed higher Chl-*a* values at the end of the experiment.

Despite the difference in Chl-*a*, phytoplankton assemblage composition, size class and growth rate under S-T+ conditions were generally similar to those observed under S0T+ but opposite to those in the S-T0. This suggests the lack of additive, antagonist or synergic effects between increased temperature and reduced salinity, at least at the taxonomic level. In addition, the similar compositional response observed between S-T+ and S0T+ suggests that the impact of temperature increase on phytoplankton assemblages is stronger than that of salinity decrease. Thus, our results could be extrapolated to coastal areas presently subject to increasing water temperature even without the effect of glacial melting, or to future conditions, in which the effect of glacier melting might be reduced after intense glacier retreat.

5. Conclusion

In this study we found that the abundance of nano-sized diatoms of the genera *Chaetoceros* and *Shionodiscus* and small unidentified phytoflagellates increased in high temperature treatments, compensating the potential damaging effects of salinity, whereas micro-size pennate diatoms decreased. Moreover, an increase in the relative abundance of chlorophytes was observed only in the low salinity treatments, under nitrate depletion. Based on our results, climate change can result in a shift towards nanophytoplankton dominance in phytoplankton assemblages that could change the productivity of Antarctic ecosystems, with direct consequences to organisms at higher trophic levels. In addition, the high abundance of the temperate-water species *Chaetoceros socialis* and *Shionodiscus gaarderae* in this experiment suggests that they can be potentially dominant over cold water species in Antarctic waters. Given the observed taxa-specific responses to temperature and salinity changes in this and previous studies, monoculture studies should be conducted to identify the genetic, physiological and/or morphological characteristics that may allow the different taxa to growth under future oceanic conditions.

Funding sources

This work was supported by grants PICT 2011-130 Raíces from Agencia Nacional de Promociones Científicas (ANPCyT, Argentina) to I.R.S., and PIP-0122 from Consejo Nacional de Investigaciones Científicas y Técnicas (CONICET, Argentina) to G.O.A. and a CONICET doctoral fellowship to J.S.A. Funding from a Canadian NSERC Discovery Grant awarded to D.E.V. was used to support partial travel costs for D.E.V.

Author contribution

Julieta S. Antoni: Conceptualization, Formal analysis, Visualization, Writing - Original Draft, Writing - Review & Editing. **Gastón O. Almandoz**: Conceptualization, Formal analysis, Writing - Original Draft, Writing - Review & Editing, Supervision. **Martha E. Ferrario**: Data curation, Formal analysis, Writing - Review & Editing. **Marcelo P. Hernando**: Conceptualization, Methodology, Writing - Original Draft, Writing - Review & Editing. **Diana E. Varela**: Conceptualization, Methodology, Writing - Review & Editing. **Patrick D. Rozema**: Formal analysis, Writing - Review & Editing. **Anita G.J. Buma**: Formal analysis, Writing - Review & Editing. **Flavio E. Paparazzo**: Formal analysis, Writing - Review & Editing. **Irene R. Schloss**: Conceptualization, Formal analysis, Methodology, Writing - Original Draft, Writing - Review & Editing, Supervision.

Declaration of Competing Interest

The authors declare that they have no known competing financial interests or personal relationships that could have appeared to influence the work reported in this paper.

Acknowledgements

This research was also supported by EU FP7-People-2012-IRSES programme (IMCONet, agreement no. 318718) and is a contribution to CoastCarb (Funding ID 872609, H2020, MSCA-RISE-2019, Research and Innovation Staff Exchange). We thank Diego Giménez (IDEA-CONICET) and Gwenaëlle Gremion (ISMER-UQAR, Rimouski, Canada) for their assistance during the experiments, as well as the personnel of the Carlini Station and the divers of the Prefectura Naval Argentina for their help during field work.

Appendix A. Supplementary data

Supplementary data to this article can be found online at https://doi.org/10.1016/j.jembe.2020.151444.

References

Aksnes, D.L., Egge, J.K., 1991. A theoretical model for nutrient uptake in phytoplankton. Mar. Ecol. Prog. Ser. 70, 65–72.

Almandoz, G.O., Ferreyra, G.A., Schloss, I.R., Dogliotti, A.I., Rupolo, V., Paparazzo, F.E., Esteves, J.L., Ferrario, M.E., 2008. Distribution and ecology of *Pseudo-nitzschia* species (Bacillariophyceae) in surface waters of the Weddell Sea (Antarctica). Polar Biol. 31, 429–442.

Alverson, A.J., Kang, S.H., Theriot, E.C., 2006. Cell wall morphology and systematic importance of *Thalassiosira ritscheri* (Hustedt) Hasle, with a description of Shionodiscus gen. nov. Diatom. Res. 21, 251–262.

Alves-de-Souza, C., González, M.T., Iriarte, J.L., 2008. Functional groups in marine phytoplankton assemblages dominated by diatoms in fjords of southern Chile. J. Plankton Res. 30, 1233–1243.

Arrigo, K.R., Sullivan, C.W., 1992. The influence of salinity and temperature covariation on the photophysiological characteristics of antarctic sea ice microalgae. J. Phycol. 28, 746–756.

Atkinson, D., Ciotti, B.J., Montagnes, D.J.S., 2003. Protists decrease in size linearly with temperature: ca. 2.5% C-1. Proc. R. Soc. B Biol. Sci. 270, 2605–2611.

Baardsnes, J., Jelokhani-Niaraki, M., Kondejewski, L.H., Kuiper, M.J., Kay, C.M., Hodges, R.S., Davies, P.L., 2001. Antifreeze protein from shorthorn sculpin: identification of the ice-binding surface. Protein Sci. 10, 2566–2576.

Berges, J.A., Varela, D.E., Harrison, P.J., 2002. Effects of temperature on growth rate, cell composition and nitrogen metabolism in the marine diatom *Thalassiosira pseudonana* (Bacillariophyceae). Mar. Ecol. Prog. Ser. 225, 139–146.

Booth, B.C., Larouche, P., Bélanger, S., Klein, B., Amiel, D., Mei, Z.P., 2002. Dynamics of *Chaetoceros socialis* blooms in the North Water. Deep Sea Res. Part 2 Top. Stud. Oceanogr. 49, 5003–5025.

Brucet, S., Boix, D., Quintana, X.D., Jensen, E., Nathansen, L.W., Trochine, C., Jeppesen, E., 2010. Factors influencing zooplankton size structure at contrasting temperatures in coastal shallow lakes: implications for effects of climate change. Limnol. Oceanogr. 55, 1697–1711.

Carter, C.M., Ross, A.H., Schiel, D.R., Howard-Williams, C., Hayden, B., 2005. In situ microcosm experiments on the influence of nitrate and light on phytoplankton community composition. J. Exp. Mar. Biol. Ecol. 326, 1–13.

Cefarelli, A.O., Ferrario, M.E., Almandoz, G.O., Atencio, A.G., Akselman, R., Vernet, M., 2010. Diversity of the diatom genus *Fragilariopsis* in the argentine sea and Antarctic waters: morphology, distribution and abundance. Polar Biol. 33, 1463–1484.

Chamnansinp, A., Li, Y., Lundholm, N., Moestrup, Ø., 2013. Global diversity of two widespread, colony-forming diatoms of the marine plankton, *Chaetoceros socialis* (syn. *C. radians*) and *Chaetoceros gelidus* sp. nov. J. Phycol. 49, 1128–1141.

Chown, S.L., Clarke, A., Fraser, C.I., Cary, S.C., Moon, K.L., McGeoch, M.A., 2015. The changing form of Antarctic biodiversity. Nature 522, 431.

Clarke, A., Murphy, E.J., Meredith, M.P., King, J.C., Peck, L.S., Barnes, D.K.A., Smith, R.C., 2007. Climate change and the marine ecosystem of the western Antarctic peninsula. Philos. Trans. R. Soc. B. Biol. Sci. 362, 149–166.

Coello-Camba, A., Agustí, S., Vaqué, D., Holding, J., Arrieta, J.M., Wassmann, P., Duarte, C.M., 2015. Experimental assessment of temperature thresholds for Arctic

phytoplankton communities. Estuar. Coasts 38, 873–885.
Cohen, J.E., Jonsson, T., Carpenter, S.R., 2003. Ecological community description using the food web, species abundance, and body size. Proc. Natl. Acad. Sci. 100, 1781–1786.
Convey, P., Bindschadler, R., Di Prisco, G., Fahrbach, E., Gutt, J., Hodgson, D.A., others, 2009. Antarctic climate change and the environment. Antarct. Sci. 21, 541–563.
Daufresne, M., Lengfellner, K., Sommer, U., 2009. Global warming benefits the small in aquatic ecosystems. Proc. Natl. Acad. Sci. 106, 12788–12793.
De Jong, J., Schoemann, V., Lannuzel, D., Croot, P., de Baar, H., Tison, J.L., 2012. Natural iron fertilization of the Atlantic sector of the Southern Ocean by continental shelf sources of the Antarctic peninsula. J. Geophys. Res. 117, G01029. https://doi.org/10.1029/2011JG001679.
Eicken, H., 1992. The role of sea ice in structuring Antarctic ecosystems. Polar Biol. 12, 3–13.
Eppley, R.W., 1972. Temperature and phytoplankton growth in the sea. Fish. Bull. 70, 1063–1085.
Eppley, R.W., Thomas, W.H., 1969. Comparison of half-saturation constants for growth and nitrate uptake of marine phytoplankton. J. Phycol. 5, 375–379.
Falkowski, P.G., Barber, R.T., Smetacek, V., 1998. Biogeochemical controls and feedbacks on ocean primary production. Science 281, 200–206.
Ferrario, M.E., Sar, E.A., Sala, S.E., 1995. Metodología básica para el estudio del fitoplancton con especial referencia a las diatomeas. In: Alvear, K., Ferrario, M.E., Oliveira, E.C., Sar, E.A. (Eds.), Manual de métodos ficológicos. Universidad de Concepción, Concepción, pp. 1–23.
Ferrario, M.E., Almandoz, G.O., Cefarelli, A.O., Beszteri, B., Akselman, R., Fabro, E., Cembella, A., 2018. *Shionodiscus gaarderae* sp. nov. (Thalassiosirales, Thalassiosiraceae), a bloom–producing diatom from the southwestern Atlantic Ocean, and emendation of *Shionodiscus bioculatus* var. *bioculatus*. Diatom. Res. 33, 25–37.
Fiala, M., Kuosa, H., Kopczyńska, E.E., Oriol, L., Delille, D., 2006. Spatial and seasonal heterogeneity of sea ice microbial communities in the first–year ice of Terre Adélie area (Antarctica). Aquat. Microb. Ecol. 43, 95–106.
Finkel, Z.V., Beardall, J., Flynn, K.J., Quigg, A., Rees, T.A.V., Raven, J.A., 2010. Phytoplankton in a changing world: cell size and elemental stoichiometry. J. Plankton Res. 32, 119–137.
Frost, B.W., 1972. Effects of size and concentration of food particles on the feeding behavior of the marine planktonic copepod *Calanus pacificus*. Limnol. Oceanogr. 17, 805–815.
Gao, Y., Smith, G.J., Alberte, R.S., 2000. Temperature dependence of nitrate reductase activity in marine phytoplankton: biochemical analysis and ecological implications. J. Phycol. 313, 304–313.
Gao, G., Jin, P., Liu, N., Li, F., Tong, S., Hutchins, D.A., Gao, K., 2017. The acclimation process of phytoplankton biomass, carbon fixation and respiration to the combined effects of elevated temperature and pCO2 in the northern South China Sea. Mar. Pollut. Bull. 118, 213–220. https://doi.org/10.1016/j.marpolbul.2017.02.063.
García Valenzuela, X., García Moya, E., Rascón Cruz, Q., Herrera Estrella, L., Aguado Santacruz, G.A., 2005. Chlorophyll accumulation is enhanced by osmotic stress in graminaceous chlorophyllic cells. J. Plant Physiol. 162, 650–661.
Gardner, J.L., Peters, A., Kearney, M.R., Joseph, L., Heinsohn, R., 2011. Declining body size: a third universal response to warming? Trends Ecol. Evol. 26, 285–291.
Garibotti, I.A., Vernet, M., Ferrario, M.E., Smith, R.C., Ross, R.M., Quetin, L.B., 2003. Phytoplankton spatial distribution patterns along the western Antarctic peninsula (Southern Ocean). Mar. Ecol. Prog. Ser. 261, 21–39.
Gilmour, D.J., Hipkins, M.F., Boney, A.D., 1984. The effect of decreasing the external salinity on the primary processes of photosynthesis in *Dunaliella tertiolecta*. J. Exp. Bot. 35, 28–35.
Gleitz, M., Loeff, M. Rvd, Thomas, D.N., Dieckmann, G.S., Miller, F.J., 1995. Comparison of summer and winter inorganic carbon, oxygen and nutrient concentrations in Antarctic Sea ice brine. Mar. Chem. 51, 81–91.
Grover, J.P., 1991. Resource competition in a variable environment: phytoplankton growing according to the variable–internal–stores model. Am. Nat. 138, 811–835.
Günther, S., Dieckmann, G.S., 2001. Vertical zonation and community transition of sea–ice diatoms in fast ice and platelet layer, Weddell Sea, Antarctica. Ann. Glaciol. 33, 287–296.
Gutt, J., Bertler, N., Bracegirdle, T.J., Buschmann, A., Comiso, J., Hosie, G., Isla, E., Schloss, I.R., Smith, C.R., Tournadre, J., Xavier, J.C., 2015. The Southern Ocean ecosystem under multiple climate change stresses – an integrated circumpolar assessment. Glob. Chang. Biol. 211, 434–1453.
Hare, C.E., Leblanc, K., DiTullio, G.R., Kudela, R.M., Zhang, Y., Lee, P.A., ... Hutchins, D.A., 2007. Consequences of increased temperature and CO_2 for phytoplankton community structure in the Bering Sea. Mar. Ecol. Prog. Ser. 352, 9–16.
Hasle, G.R., Syvertsen, E.E., 1997. Marine Diatoms. In: Tomas, C.R. (Ed.), Identifying Marine Phytoplankton. Academic, San Diego, pp. 5–385.
Hein, M., Pedersen, M.F., Sand Jensen, K., 1995. Size–dependent nitrogen uptake in micro–and macroalgae. Mar. Ecol. Prog. Ser. 118, 247–253.
Hernando, M., Schloss, I.R., Malanga, G., Almandoz, G.O., Ferreyra, G.A., Aguiar, M.B., Puntarulo, S., 2015. Effects of salinity changes on coastal Antarctic phytoplankton physiology and assemblage composition. J. Exp. Mar. Biol. Ecol. 466, 110–119.
Hernando, M., Schloss, I.R., Almandoz, G.O., Malanga, G., Varela, D.E., De Troch, M., 2018. Combined effects of temperature and salinity on fatty acid content and lipid damage in Antarctic phytoplankton. J. Exp. Mar. Biol. Ecol. 503, 120–128.
Higgins, H.H.W., Wright, S.W., Schlűter, L., Schlüter, L., 2012. Quantitative interpretation of chemotaxonomic pigment data. In: Roy, S., Llewellyn, C.A., Egeland, E.S., Johnsen, G. (Eds.), Phytoplankton Pigments: Characterization, Chemotaxonomy and Applications in Oceanography. Cambridge University Press, pp. 257–313.
Holm-Hansen, O., Riemann, B., 1978. Chlorophyll a determination: improvements in methodology. Oikos 30, 438–447.
Holm-Hansen, O., Lorenzen, C.J., Holmes, R.W., Strickland, J.D., 1965. Fluorometric determination of chlorophyll. J. Cons. Int. Explor. Mer 30, 3–15.
IPCC, 2019. Summary for policymakers. In: Pörtner, H.-O., Roberts, D.C., Masson-Delmotte, V., Zhai, P., Tignor, M., Poloczanska, E. ... Weyer, N. (Eds.), IPCC Special Report on the Ocean and Cryosphere in a Changing Climate, (In press).
IPCC 2007, Solomon, S., Manning, M., Marquis, M., Qin, D., 2007. Climate Change 2007-the Physical Science Basis: Working Group I Contribution to the Fourth Assessment Report of the IPCC. 4 Cambridge University Press.
Irwin, A.J., Finkel, Z.V., Schofield, O.M.E., Falkowski, P.G., 2006. Scaling–up from nutrient physiology to the size–structure of phytoplankton communities. J. Plankton Res. 28, 459–471.
Ishikawa, A., Wright, S.W., van den Enden, R., Davidson, A.T., Marchant, H.J., 2002. Abundance, size structure and community composition of phytoplankton in the Southern Ocean in the austral summer 1999/2000. Polar Biosci. 15, 11–26.
Kang, S.H., Kang, J.S., Lee, S., Chung, K.H., Kim, D., Park, M.G., 2001. Antarctic phytoplankton assemblages in the marginal ice zone of the northwestern Weddell Sea. J. Plankton Res. 23, 333–352.
Kim, H., Ducklow, H.W., Abele, D., Ruiz Barlett, E.M., Buma, A.G., Meredith, M.P., others, 2018. Inter–decadal variability of phytoplankton biomass along the coastal West Antarctic Peninsula. Philos. Trans. A Math. Phys. Eng. Sci. 376, 20170174.
Kopczyńska, E.E., 2008. Phytoplankton variability in Admiralty Bay, King George Island, South Shetland Islands: six years of monitoring. Pol. Polar Res. 29, 117–139.
Kremp, A., Godhe, A., Egardt, J., Dupont, S., Suikkanen, S., Casabianca, S., Penna, A., 2012. Intraspecific variability in the response of bloom–forming marine microalgae to changed climate conditions. Ecol. Evol. 21, 195–1207.
Lange, P.K., Tenenbaum, D.R., Santis Braga, E., Campos, L.S., 2007. Microphytoplankton assemblages in shallow waters at Admiralty Bay (King George Island, Antarctica) during the summer 2002–2003. Polar Biol. 30, 1483–1492.
Lee, Y.C., Park, M.O., Jung, J., Yang, E.J., Lee, S.H., 2016. Taxonomic variability of phytoplankton and relationship with production of CDOM in the polynya of the Amundsen Sea, Antarctica. Deep Sea Res. Part 2 Top. Stud. Oceanogr. 123, 30–41.
Lewandowska, A.M., Boyce, D.G., Hofmann, M., Matthiessen, B., Sommer, U., Worm, B., 2014a. b. Effects of sea surface warming on marine plankton. Ecol. Lett. 17, 614–623.
Lewandowska, A.M., Hillebrand, H., Lengfellner, K., Sommer, U., 2014b. a. Temperature effects on phytoplankton diversity – the zooplankton link. J. Sea Res. 85, 359–364.
Li, W.K., McLaughlin, F.A., Lovejoy, C., Carmack, E.C., 2009. Smallest algae thrive as the Arctic Ocean freshens. Science 326 (539–539).
Lizotte, M.P., 2001. The contributions of sea ice algae to Antarctic marine primary production. Am. Zool. 41, 57–73.
Lomas, M.W., Glibert, P.M., 2000. Comparisons of nitrate uptake, storage, and reduction in marine diatoms and flagellates. J. Phycol. 36, 903–913.
Lundholm, N., Hasle, G.R., 2008. Are *Fragilariopsis cylindrus* and *Fragilariopsis nana* bipolar diatoms?–morphological and molecular analyses of two sympatric species. Nova Hedwig. Beih. 133, 231–250.
Mackey, M.D., Mackey, D.J., Higgins, H.W., Wright, S.W., 1996. CHEMTAX –a program for estimating class abundances from chemical markers: application to HPLC measurements of phytoplankton. Mar. Ecol. Prog. Ser. 144, 265–283.
Marañón, E., Cermeño, P., Latasa, M., Tadonléké, R.D., 2012. Temperature, resources, and phytoplankton size structure in the ocean. Limnol. Oceanogr. 5, 1266–1278.
Maykut, G.A., 1986. The surface heat and mass balance. In: Untersteiner, N. (Ed.), The Geophysics of Sea Ice. NATO–AS1Senes B: Physics. 146. Plenum Press, New York, pp. 395–464.
McLachlan, J., 1961. The effect of salinity on growth and chlorophyll content in representative classes of unicellular marine algae. Can. J. Microbiol. 7, 399–406.
McMinn, A., Hodgson, D., 1993. Summer phytoplankton succession in Ellis Fjord, eastern Antarctica. J. Plankton Res. 15, 925–938.
Mendes, C.R.B., Tavano, V.M., Leal, M.C., de Souza, M.S., Brotas, V., Garcia, C.A.E., 2013. Shifts in the dominance between diatoms and cryptophytes during three late summers in the Bransfield Strait (Antarctic peninsula). Polar Biol. 36, 537–547.
Meredith, M.P., Stefels, J., van Leeuwe, M., 2017. Marine studies at the western Antarctic peninsula: priorities, progress and prognosis. Deep Sea Res. Part 2 Top. Stud. Oceanogr. 139, 1–8.
Meredith, M.P., Falk, U., Bers, A.V., Mackensen, A., Schloss, I.R., Barlett, E.R., Jerosch, K., Busso, A.S., Abele, D., 2018. Anatomy of a glacial meltwater discharge event in an Antarctic cove. Philos. Trans. A Math. Phys. Eng. Sci. 376, 20170163.
Millero, F.J., 2016. Chemical Oceanography. CRC press.
Mock, T., Krell, A., Glöckner, G., Kolukisaoglu, Ü., Valentin, K., 2006. Analysis of expressed sequence tags (ests) from the polar diatom *Fragilariopsis cylindrus*. J. Phycol. 42, 78–85.
Moisan, T.A., Fryxell, G.A., 1993. The distribution of Antarctic diatoms in the Weddell Sea during austral winter. Bot. Mar. 36, 489–498.
Moline, M.A., Prézelin, B.B., 1996. Long–term monitoring and analyses of physical factors regulating variability in coastal Antarctic phytoplankton biomass, in situ productivity and taxonomic composition over subseasonal, seasonal and interannual time scales. Mar. Ecol. Prog. Ser. 145, 143–160.
Moline, M.A., Claustre, H., Frazer, T.K., Grzymski, J., Vernet, M., 2001. Changes in phytoplankton assemblages along the Antarctic peninsula and potential implications for the Antarctic food web. In: Davison, W., Howard Williams, C., Brody, P. (Eds.), Antarctic Ecosystems: Model for Wider Ecological Understanding. Caxton Press, Christchurch, pp. 263–271.
Montes Hugo, M., Doney, S.C., Ducklow, H.W., Fraser, W., Martinson, D., Stammerjohn, S.E., Schofield, O., 2009. Recent changes in phytoplankton communities associated with rapid regional climate change along the western Antarctic peninsula. Science. 323, 1470–1473.
Morán, X.A.G., López-Urrutia, A., Calvo-Díaz, L., Li, W.K.W., 2010. Increasing importance

of small phytoplankton in a warmer ocean. Glob. Chang. Biol. 16, 1137–1144.
Mousing, E.A., Ellegaard, M., Richardson, K., 2014. Global patterns in phytoplankton community size structure—evidence for a direct temperature effect. Mar. Ecol. Prog. Ser. 497, 25–38.
Nelson, D.M., Ahern, J.A., Herlihy, L.J., 1991. Cycling of biogenic silica within the upper water column of the Ross Sea. Mar. Chem. 35, 461–476.
Neori, A., Holm Hansen, O., 1982. Effect of temperature on rate of photosynthesis in Antarctic phytoplankton. Polar Biol. 1, 33–38.
Ogilvie, S.C., Ross, A.H., James, M.R., Schiel, D.R., 2003. In situ enclosure experiments on the influence of cultured mussels (*Perna canaliculus*) on phytoplankton at times of high and low ambient nitrogen. J. Exp. Mar. Biol. Ecol. 295, 23–39.
Ostenfeld, C.H., 1913. On the distribution of Bacillariales (diatoms) in the plankton of the north European waters according to the international sea investigations, with special relation to hydrographical conditions. Bureau du Conseil permanent international pour l'exploration de la mer, Resumé Planktonique. Bull. Trimest. 3, 403–508.
Park, S., Ahn, I.-Y., Sin, E., Shim, J.H., Kim, T., 2020. Ocean freshening and acidification differentially influence mortality and behavior of the Antarctic amphipod *Gondogeneia antarctica*. Mar. Environ. Res. 154, 104847.
Perl, J., 2009. The SDU (CHORS) Method. In: The Third SeaWiFS HPLC Analysis Round–Robin Experiment (SeaHARRE–3) (NASA). pp. 89–91.
Peter, K.H., Sommer, U., 2012. Phytoplankton cell size: intra-and interspecific effects of warming and grazing. PLoS One 7https://doi.org/10.1371/journal.pone.0049632. e49632.
Petrou, K., Doblin, M.A., Ralph, P.J., 2011. Heterogeneity in the photoprotective capacity of three Antarctic diatoms during short–term changes in salinity and temperature. Mar. Biol. 158, 1029–1041.
Prygiel, J., Coste, M., 2000. Guide méthodologique pour la mise en oeuvre de l'Indice Biologique Diatomées NF T 90–354. In: Agences de l'Eau, Ministere de l'Aménagement Du Territoire et de l'Environnement, Cemagref, Paris, France.
Ralph, P.J., McMinn, A., Ryan, K.G., Ashworth, C., 2005. Short–term effect of temperature on the photokinetics of microalgae from the surface layers of Antarctic pack ice. J. Phycol. 41, 763–769.
Rines, J.E.B., Hargraves, P.E., 1988. The *Chaetoceros* Ehrenberg (Bacillariophyceae) flora of Narragansett Bay, Rhode Island, USA. Bibl. Phycol. 79, 5–196.
Rozema, P.D., Venables, H.J., van de Poll, W.H., Clarke, A., Meredith, M.P., Buma, A.G.J., 2017. Interannual variability in phytoplankton biomass and species composition in northern Marguerite Bay (West Antarctic peninsula) is governed by both winter sea ice cover and summer stratification. Limnol. Oceanogr. 62, 235–252.
Rüger, T., Sommer, U., 2012. Warming does not always benefit the small – results from a plankton experiment. Aquat. Bot. 97, 64–68.
Scheiner, S.M., 2001. MANOVA: Multiple response variables and multispecies interactions. In: Scheiner, Gurevitch (Ed.), Design and Analysis of Ecological Experiments, 2nd ed. Oxford Univ. Press, Oxford.
Schloss, I.R., 1997. Escalas temporo-espaciales de variabilidad del fitoplancton costero antártico (Doctoral dissertation, Universidad de Buenos Aires. Facultad de Ciencias Exactas y Naturales).
Schloss, I.R., Ferreyra, G.A., 2002. Primary production, light and vertical mixing in Potter Cove, a shallow bay in the maritime Antarctic. Polar Biol. 25, 41–48.
Schloss, I.R., Abele, D., Moreau, S., Demers, S., Bers, A.V., González, O., Ferreyra, G.A., 2012. Response of phytoplankton dynamics to 19-year (1991–2009) climate trends in Potter Cove (Antarctica). J. Mar. Syst. 92, 53–66.
Schloss, I., Wasilowska, A., Dumont, D., Almandoz, G.O., Hernando, M.P., Saravia, L., Ferreyra, G., 2014. On the phytoplankton bloom in coastal waters of southern King George Island (Antarctica) in January 2010 : An exceptional feature? Limnol. Oceanogr. 59, 195–210.
Schofield, O., Saba, G., Coleman, K., Carvalho, F., Couto, N., Ducklow, H., Finkel, Z., Irwin, A., Kahl, A., Miles, T., Montes–Hugo, M., Stammerjohn, S., Waite, N., 2017. Decadal variability in coastal phytoplankton community composition in a changing West Antarctic peninsula. Deep Sea Res. Part 1 (124), 42–54.
Scott, F.J., Marchant, H.J., 2005. Antarctic Marine Protists. Australian Biological Resources Study, Hobart. Australian Antarctic Division, Canberra.
Scott, P., McMinn, A., Hosie, G., 1994. Physical parameters influencing diatom community structure in eastern Antarctic Sea ice. Polar Biol. 14, 507–517.
Shuter, B.J., 1978. Size dependence of phosphorus and nitrogen subsistence quotas in unicellular microorganisms. Limnol. Oceanogr. 23, 1248–1255.
Simões, J.C., Bremer, U.F., Aquino, F.E., Ferron, F.A., 1999. Morphology and variations of glacial drainage basins in the King George Island ice field, Antarctica. Ann. Glaciol. 29, 220–224.
Skalar Analytical® V.B, 2005a. a. Skalar Methods - Analysis: Nitrate + Nitrite - Catnr. 461–031 + DIAMOND issue 081505/MH/99235956. Breda (The Netherlands).
Skalar Analytical® V.B, 2005b. b. Skalar Methods - Analysis: Phosphate - Catnr. 503-010w/r + DIAMOND issue 081505/MH/99235956. Breda (The Netherlands).
Skalar Analytical® V.B, 2005c. c. Skalar Methods - Analysis: Silicate -Catnr. 563–051 + DIAMOND issue 081505/MH/99235956. Breda (The Netherlands).
Skau, L.F., Andersen, T., Thrane, J.E., Hessen, D.O., 2017. Growth, stoichiometry and cell size; temperature and nutrient responses in haptophytes. PeerJ. 5, e3743. https://doi.org/10.7717/peerj.3743.
Smetacek, V., Assmy, P., Henjes, J., 2004. The role of grazing in structuring Southern Ocean pelagic ecosystems and biogeochemical cycles. Antarct. Sci. 16, 541–558.
Søgaard, D.H., Hansen, P.J., Rysgaard, S., Glud, R.N., 2011. Growth limitation of three Arctic Sea ice algal species: effects of salinity, pH, and inorganic carbon availability. Polar Biol. 34, 1157–1165.
Tagliabue, A., Bopp, L., Aumont, O., 2009. Evaluating the importance of atmospheric and sedimentary iron sources to Southern Ocean biogeochemistry. Geophys. Res. Lett. 36.
Teoh, M.L., Chu, W.L., Marchant, H., Phang, S.M., 2004. Influence of culture temperature on the growth, biochemical composition and fatty acid profiles of six Antarctic microalgae. J. Appl. Phycol. 16, 421–430.
Tragin, M., Vaulot, D., 2018. Green microalgae in marine coastal waters: the ocean sampling day (OSD) dataset. Sci. Rep. 8, 1–12. https://doi.org/10.1038/s41598-018-32338-w.
Trathan, P.N., Forcada, J., Murphy, E.J., 2007. Environmental forcing and Southern Ocean marine predator populations: effects of climate change and variability. Philos. Trans. R. Soc. B Biol. Sci. 362, 2351–2365.
Turner, J., Colwell, S.R., Marshall, G.J., Lachlan Cope, T.A., Carleton, A.M., Jones, P.D., Lagun, V., Reid, P.A., Iagovkina, S., 2005. Antarctic climate change during the last 50 years. Int. J. Climatol. 25, 279–294.
Turner, J., Barrand, N.E., Bracegirdle, T.J., Convey, P., Hodgson, D.A., Jarvis, M., Shanklin, J., 2014. Antarctic climate change and the environment: an update. Polar Rec. 50, 237–259.
Utermöhl, H., 1958. Zur Vervollkommnung der quantitativen phytoplankton Methodik. Mitt. Int. Ver. Theor. Angew. Limnol. 9, 1–38.
van de Poll, W.H., Lagunas, M., de Vries, T., Visser, R.J., Buma, A.G., 2011. Non–photochemical quenching of chlorophyll fluorescence and xanthophyll cycle responses after excess PAR and UVR in *Chaetoceros brevis*, *Phaeocystis antarctica* and coastal Antarctic phytoplankton. Mar. Ecol. Prog. Ser. 426, 119–131.
VanHeukelem, L., Thomas, C.S., 2001. Computer–assisted high–performance liquid chromatography method development with applications to the isolation and analysis of phytoplankton pigments. J. Chromatogr. A 910, 31–49. https://doi.org/10.1016/S0378–4347(00)00603–4.
Vaughan, D.G., Marshall, G.J., Connolley, W.M., Parkinson, C., Mulvaney, R., Hodgson, D.A., others, 2003. Recent rapid regional climate warming on the Antarctic peninsula. Clim. Chang. 60, 243–274.
Waite, A., Fisher, A., Thompson, P.A., Harrison, P.J., 1997. Sinking rate versus cell volume relationships illuminate sinking rate control mechanisms in marine diatoms. Mar. Ecol. Prog. Ser. 157, 97–108.
Wang, X., Tang, K.W., Wang, Y., Smith, W.O., 2010. Temperature effects on growth, colony development and carbon partitioning in three *Phaeocystis* species. Aquat. Biol. 9, 239–249.
Ward, B.A., 2015. Temperature-correlated changes in phytoplankton community structure are restricted to polar waters. PLoS One 10, e0135581. https://doi.org/10.1371/journal.pone.0135581.
Wright, S.W., Ishikawa, A., Marchant, H.J., Davidson, A.T., van den Enden, R.L., Nash, G.V., 2009. Composition and significance of picophytoplankton in Antarctic waters. Polar Biol. 32, 797–808. https://doi.org/10.1007/s00300–009–0582–9.
Wright, S.W., van den Enden, R.L., Pearce, I., Davidson, A.T., Scott, F.J., Westwood, K.J., 2010. Phytoplankton community structure and stocks in the Southern Ocean (30–80°E) determined by CHEMTAX analysis of HPLC pigment signatures. Deep Sea Res. Part 2 Top. Stud. Oceanogr. 57, 758–778. https://doi.org/10.1016/j.dsr2.2009.06.015.
Zhu, Z., Qu, P., Gale, J., Fu, F., Hutchins, D.A., 2017. Individual and interactive effects of warming and CO2 on *Pseudo-nitzschia subcurvata* and *Phaeocystis antarctica*, two dominant phytoplankton from the Ross Sea, Antarctica. Biogeosciences 14, 5281–5295.